

1 **In-situ and Denuder Based Measurements of Elemental and Reactive**
2 **Gaseous Mercury with Analysis by Laser-Induced Fluorescence. Results**
3 **from the Reno Atmospheric Mercury Intercomparison Experiment.**

4 Anthony J. Hynes^{*}, Stephanie Everhart, Dieter Bauer, James Remeika, and Cheryl Tatum
5 Ernest¹

6 Division of Marine and Atmospheric Chemistry, Rosenstiel School of Marine and
7 Atmospheric Science, University of Miami, 4600 Rickenbacker Causeway, Miami,
8 Florida 33149

9 ¹current address: Atmospheric Chemistry Department, Max Planck Institute for
10 Chemistry, Hahn-Meitner-Weg 1, Mainz, 55128, Germany

11 ^{*} Corresponding author. Tel.: +1-305-421-4173; fax: +1-305-421-4689. E-mail address:
12 ahynes@rsmas.miami.edu (A. J. Hynes)

13
14 **Abstract**

15 The University of Miami (UM) deployed a sequential two photon laser-induced fluorescence (2P-LIF)
16 instrument for the in-situ measurement of gaseous elemental mercury, Hg(0), during the Reno Atmospheric
17 Mercury Intercomparison Experiment (RAMIX) campaign. A number of extended sampling experiments,
18 typically lasting 6-8 hours but on one occasion extending to ~24 hours, were conducted allowing the 2P-
19 LIF measurements of Hg(0) concentrations to be compared with two independently operated instruments
20 using gold amalgamation sampling coupled with Cold Vapor Atomic Fluorescence Spectroscopic (CVAFS)
21 analysis. At the highest temporal resolution, ~5 minute samples, the three instruments measured
22 concentrations that agreed to within 10-25%. Measurements of total mercury (TM) were made by using
23 pyrolysis to convert total oxidized mercury (TOM) to Hg(0). TOM was then obtained by difference.
24 Variability in the ambient Hg(0) concentration limited our sensitivity for measurement of ambient TOM
25 using this approach. In addition, manually sampled KCl coated annular denuders were deployed and
26 analyzed using thermal dissociation coupled with single photon LIF detection of Hg(0). The TOM
27 measurements obtained were normally consistent with KCl denuder measurements obtained with two
28 Tekran speciation systems and with the manual KCl denuder measurements but with very large uncertainty.
29 They were typically lower than measurements reported by the University of Washington (UW) Detector for
30 Oxidized Hg Species (DOHGS) system. The ability of the 2P-LIF pyrolysis system to measure TM was
31 demonstrated during one of the manifold HgBr₂ spikes but the results did not agree well with those reported
32 by the DOHGS system. The limitations of the RAMIX experiment and potential improvements that should
33 be implemented in any future mercury instrument intercomparison are discussed. We suggest that
34 instrumental artifacts make a substantial contribution to the discrepancies in the reported measurements

35 over the course of the RAMIX campaign. This suggests that caution should be used in drawing significant
36 implications for the atmospheric cycling of mercury from the RAMIX results.

37
38

39

40 **1.0 Introduction:**

41 The environmental and health impacts of mercury pollution are well recognized with impacts on
42 human health and broader environmental concerns (U.S. EPA., 2000; UNEP, 2013; Mergler et al. 2007;
43 Diez, 2009; Scheuhammer et al., 2007). There have been extensive reviews of global emissions,
44 measurements and biogeochemical cycling of mercury (Mason, 2009; Streets et al., 2011; Pirrone et al.
45 2009; Lindberg et al., 2007; Ebinghaus et al., 2009; Sprovieri et al., 2010; Selin, 2009). The concerns
46 associated with the mercury problem have resulted in attempts to regulate and control emissions at both
47 national and international levels. The latest attempt in the United States is incorporated in the Mercury and
48 Air Toxics Standards (Houyoux, and Strum, 2011; US EPA, 2013) and international efforts by the United
49 Nations Environment Program have led to the Minamata Convention on Mercury, a global
50 legally binding treaty on mercury controls (UNEP, 2008; UNEP, 2013; UNEP, 2014).
51 There is a reasonable consensus on typical background concentrations of atmospheric mercury, which are
52 extremely low. Typical concentrations range from 1.2–1.4 ng m⁻³ in the Northern Hemisphere and 0.9–1.2
53 ng m⁻³ in the Southern Hemisphere and appear to be decreasing (Slemr et al., 2011; Sprovieri et al., 2016) [
54 1 ng m⁻³ is ~ 3x10⁶ atoms cm⁻³ or ~ 120 ppq (parts per quadrillion)]. Until recently it has been accepted
55 that most of the mercury found in the boundary layer is elemental mercury, Hg(0) (Lindberg et al., 2007).
56 Oxidized or reactive gaseous mercury (RGM), normally assumed to be in the Hg(II) oxidation state, has not
57 been chemically identified and is thought to constitute a very small fraction of the total mercury
58 concentration although recent work (Gustin et al., 2013; Ambrose et al., 2013) challenges this view. Our
59 overall understanding of the atmospheric chemistry of mercury and the detailed elementary chemical
60 reactions that oxidize Hg(0) is poor (Lin et al., 2006; Hynes et al., 2009; Subir et al., 2012) and the
61 uncertainty of both the chemical identity and measurements of speciated oxidized mercury places few
62 constraints on models. Atmospheric measurements of mercury represent a significant challenge in ultra-
63 trace analytical chemistry and the issues associated with current techniques have been discussed by Gustin
64 and Jaffe (2010). We have developed a laser-based sensor for the detection of Hg(0) using sequential two-
65 photon laser-induced fluorescence (2P-LIF) (Bauer et al., 2002; Bauer et al. 2014). The instrument is
66 capable of fast, in-situ, measurement of Hg(0) at ambient levels. By incorporating pyrolysis to convert
67 RGM and particulate mercury to Hg(0) it is possible to measure total mercury (TM, i.e. the sum of Hg(0)
68 plus gas phase and particulate bound oxidized mercury) and hence to measure total oxidized mercury
69 (TOM, i.e. the sum of gas phase and particulate bound oxidized mercury) by difference. The Reno
70 Atmospheric Mercury Intercomparison Experiment (RAMIX) offered an opportunity to deploy the 2P-LIF
71 instrument as part of an informal field intercomparison at the University of Nevada Agricultural
72 Experiment Station (Gustin et al., 2013; Ambrose et al., 2013; Finley et al., 2013). RAMIX was an attempt

73 to intercompare new Hg measurement systems with two Tekran 2537/1130/1135 systems. This is the
74 instrumentation that is currently in use for the overwhelming majority of atmospheric Hg measurements.
75 Participants included the University of Washington (UW), University of Houston (UH), Desert Research
76 Institute (DRI), University of Nevada Reno (UNR) and the University of Miami (UM). The specific goals
77 for the project were:

- 78 1- Compare ambient measurements of gaseous elemental mercury, Hg(0), gaseous oxidized mercury
79 (RGM) and particulate bound mercury (PBM) by multiple groups for 4 weeks.
- 80 2- Examine the response of all systems to spikes of Hg(0) and HgBr₂.
- 81 3- Examine the response of all systems to Hg(0) in the presence of the potentially interfering
82 compounds ozone and water vapor.
- 83 4- Analyze the data to quantify the level of agreement and the results of interference and calibration
84 tests for each measurement system.

85 In practice the instrument operated by UH only measured Hg(0) for the first week of the campaign and the
86 cavity ring down spectroscopy (CRDS) instrument deployed by DRI did not produce any data. Hence
87 RAMIX was primarily an intercomparison of the UM 2P-LIF instrument, the UW Detector for Oxidized
88 Hg Species (DOHGS) that is based on two Tekran 2537 instruments, and a Tekran 2537 and two
89 2537/1130/1135 speciation systems deployed by UNR. Under these circumstances we were not able to
90 compare 2P-LIF measurements made at high temporal resolution with the CRDS instrument. It did allow us
91 to compare the 2P-LIF sensor with independently operated instruments that use preconcentration on gold
92 coupled with analysis by CVAFS and to examine potential interference effects. Our focus here is to
93 compare the short term variation in GEM on the timescale that the CVAFS instruments operate, ~ 5 minute
94 samples, and examine the ability of the different instruments to capture this variation. In addition, we made
95 measurements of TM and hence TOM by difference and also employed manual denuder measurements to
96 attempt to measure RGM directly. In prior publications, Gustin et al. (2013) and Ambose et al. (2013)
97 provide their interpretation of the RAMIX results and their conclusions have very significant implications
98 for our understanding of atmospheric mercury chemistry. In this work we offer a contrasting view with
99 different conclusions.

100 **2.0 Experimental**

101 **2.1 RAMIX Intercomparison.** A detailed description of the RAMIX location and the local meteorology
102 was provided by Gustin et al. (2013). The original RAMIX proposal included participation from Tekran
103 Corporation to build and test a field-deployed, high-flow sampling manifold that could be reliably spiked
104 with 10-100 parts per quadrillion of RGM. Tekran proposed to supply both RGM and Hg(0) spiking using
105 independent generators that were traceable to NIST standards and would be independent of the detection
106 systems being evaluated. However, due to time constraints Tekran believed that it was unlikely that the
107 manifold and ultra-trace spiking system could be manufactured and fully tested to their standards, so they
108 declined to participate in RAMIX (Prestbo, 2016). Instead, the UW group stepped in to supply and
109 operate the sampling manifold and spiking system and the details of its characterization are provided in

110 Finley et al. (2013). During the RAMIX campaign the 2P-LIF instrument sampled on 18 days, typically
111 sampling for between 4 and 6 hours. The longest period of continuous sampling lasted for 26 hours and
112 occurred on September 1st and 2nd. Over this 18 day period we sampled from the RAMIX manifold and, in
113 addition, at the end of the campaign we sampled ambient air independently and also attempted to measure
114 TOM by pyrolyzing the sample air and measuring the difference between Hg(0) and TM. We also sampled
115 RGM using KCl coated annular denuders using LIF for real-time analysis.

116 **2.2 The 2P-LIF system**

117 Bauer et al. (2002, 2003, 2014) provide a description of the operating principles of the 2P-LIF
118 instrument. Bauer et al. (2014) provide a detailed description of the 2P-LIF instrument deployed at RAMIX
119 including the sampling configurations, data processing, calibration and linearity tests together with
120 examples of experimental data. In summary, the system uses sequential two-photon excitation of two
121 atomic transitions in Hg(0) followed by detection of blue shifted LIF. The instrumental configuration at
122 RAMIX utilized an initial excitation of the Hg $6^3P_1-6^1S_0$ transition at 253.7 nm, followed by excitation to
123 the 7^1S_0 level via the $7^1S_0-6^3P_1$ transition at 407.8 nm. Both radiative decay and collisional energy transfer
124 produce population in the 6^1P_1 level. Blue shifted fluorescence was then observed on the strong $6^1P_1-6^1S_0$
125 transition at 184.9 nm using a solar blind photomultiplier tube (PMT). By using a solar blind tube that is
126 insensitive to laser scatter at the excitation wavelengths very high sensitivity is possible. The use of
127 narrowband excitation of two atomic transitions followed by detection of laser-induced fluorescence at a
128 third wavelength precludes the detection of any species other than Hg(0). The 2P-LIF instrument requires
129 calibration, so Hg(0) was also measured with a Tekran 2537B using its internal permeation source as an
130 absolute calibration. We sampled from the RAMIX manifold, which was below ambient pressure, through
131 ~25 ft of $\frac{1}{4}$ in Teflon tubing. No filter was placed on the sampling line to attempt to remove ambient RGM
132 or the HgBr₂ spikes that were periodically added to the sample flow. The sampling line was not heated and
133 was not shielded from the sun. The original RAMIX plan called for all instruments to be located close to
134 the manifold for optimal sampling. Unfortunately the positioning of the trailers at the actual site precluded
135 this and forced us to use a long sampling line. As a result, the internal pump on our Tekran was not able to
136 draw the 1.5 SLPM required for sampling and an auxiliary pump was placed on the Tekran exhaust to boost
137 the flow. Under atmospheric conditions the 2P-LIF instrument cannot detect RGM so, in principle, this
138 does not need to be removed from the sample gas. However, deposition of RGM on the sampling lines
139 followed by heterogeneous reduction to GEM could produce measurement artifacts. The limit of detection
140 for Hg(0) during RAMIX was $\sim 30 \text{ pg m}^{-3}$ for a 10 s or 100 shot average.

141

142 **2.3 Measurements of TM and TOM**

143 We attempted to use the 2P-LIF instrument to measure TM and hence TOM by difference. Although we
144 have routinely used this approach to convert HgCl₂ and HgBr₂ to Hg(0) in the laboratory, this was our first
145 attempt to measure total oxidized mercury at ambient concentrations. A second sampling line was attached
146 to the RAMIX manifold and a pyrolyzer was located directly at the manifold sampling port. The pyrolyzer

147 consisted of an ~0.6 cm o.d. quartz tube, 15 cm in length and partially filled with quartz wool. Wrapped
148 Nichrome wire encompassed an 8 cm section of tube that was heated until the quartz began to glow. The
149 high temperature inside the pyrolyzer reduces both RGM and particulate mercury in the manifold air to
150 Hg(0), which is then monitored by 2P- LIF and gives the sum of oxidized (both gaseous and particulate)
151 and elemental mercury, i.e. TM. Directly sampling from the manifold and measuring ambient Hg(0) then
152 allows the concentration of TOM to be calculated as the difference between the two signals. Both lines
153 were continuously sampled at 10 L/min and the flow to the fluorescence cell was switched between the
154 pyrolyzed and unpyrolyzed sample lines in, typically, 5 min intervals to attempt to track fluctuations in
155 [Hg(0)] that would obscure the relatively small signal increase attributable to TOM.

156 **2.4 Manual Denuder Sampling of RGM**

157 We conducted manual denuder sampling on seven afternoons during the RAMIX campaign to
158 attempt to quantify total RGM, We sampled using both KCl coated annular denuders and uncoated tubular
159 denuders that were then analyzed using programmable thermal dissociation (Ernest et al., 2013). In both
160 cases we monitored the Hg(0) that evolved during RGM decomposition, in real time using single photon
161 LIF. Only the annular denuder results are presented here. The use of denuder sampling coupled with
162 thermal dissociation has been described by Landis et al.(2002) and is used in the Tekran Model 1130
163 Mercury Speciation Units deployed during RAMIX. Air is pulled through a KCl coated annular denuder
164 which captures RGM but transmits elemental and particulate mercury. After a period of sampling, typically
165 one hour, the denuder is flushed with zero grade air and the denuder is heated to 500°C. The RGM is
166 thermally decomposed producing elemental mercury that desorbs from the denuder surface and is then
167 captured and analyzed by a Tekran 2537. The KCl coated annular denuders used here were manufactured
168 by URG Corporation and were identical to those described by Landis et al. for manual sampling. They were
169 located on top of one of the RAMIX instrument trailers a few feet from the entrance to the RAMIX
170 manifold inlet. The denuders sampled at 10 SLPM, they were not heated and the integrated
171 elutriator/acceleration jet and impactor/coupler described by Landis et al. and incorporated in the Model
172 1100 speciation unit were not placed on the denuder inlet. Hence, no type of particle filtering was used on
173 the inlets. The denuders were cleaned and recoated prior to the RAMIX deployment. Prior to sampling, the
174 denuders were cleaned by heating to 500 °C and then bagged and taken to the sampling site. After a period
175 of sampling that varied from ~1 to 4 hours, the denuders were capped, placed in sealed plastic bags, and
176 transported to the analysis lab at the University of Nevada, Reno. On most of the sampling days a single
177 denuder was opened and then immediately bagged serving as a field blank. On the final two days of
178 sampling, denuders were sampled in pairs, i.e. with two denuders connected inline so that the front denuder
179 sampled RGM and the rear denuder served as a blank and monitor of bleed-through of RGM. The blank
180 concentrations are typically low as shown in Table 1, however on September 10th the blank shows a very
181 high value that is indicative of significant contamination at some point during the cleaning or sampling
182 process. For the analysis, a flow of He passed through the denuders and then into a fluorescence cell where
183 any Hg(0) in the flow was detected by LIF. The LIF was monitored by two PMTs set to different gains to

184 increase the dynamic range of the detection system. Prior to the analysis, a known amount of mercury was
185 injected into the flow through a septum using a transfer syringe. The syringe sampled from a Tekran Model
186 2505 Mercury Vapor Primary Calibration Unit. Without disrupting the gas flow the denuder was then
187 placed in a clamshell tube furnace that had been preheated to 500°C. The evolution of the Hg(0) was
188 monitored for, typically, 5-10 minutes and after the LIF signal had returned to baseline a second calibration
189 injection was performed. A frequency doubled, Nd-Yag pumped dye laser was used to excite the Hg(0)
190 $6^3P_1-6^1S_0$ transition at 253.7 nm and resonance LIF was observed at the same wavelength. In this approach,
191 the detection PMT detects both LIF and laser scatter, hence sensitivity is limited by the ratio of intensity of
192 the LIF signal to the laser scatter. Since the 6^3P_1 level is efficiently quenched by both O₂ and N₂
193 (Breckenridge and Unemoto, 2007) the thermal analysis was performed in He buffer gas to achieve good
194 detection sensitivity. The excitation beam then passed through a reference cell that contained a steady flow
195 of Hg(0) from a permeation source. The LIF signal from the reference cell served to confirm that the laser
196 output was stable.

197 3.0 Results:

198 3.1 RAMIX Manifold

199 As noted above, the RAMIX manifold had to be constructed and tested by the UW group under tight time
200 constraints and details of its characterization are provided in Finley et al. (2013). A critique of the manifold
201 performance has been presented by Prestbo (2014) and we detail some key issues here. The manifold
202 deployed at RAMIX was a different size than the prototype tested in the laboratory. The laboratory
203 manifold showed very large variation in calculated transmission efficiencies of Hg(0) after spiking with a
204 permeation source. Finley et al. reported recoveries of 71-101% for short-term spikes. The authors
205 speculate that this was associated with rapid changes in ambient Hg(0) but provide no measurements to
206 support this. The Hg(0) source used for spiking was gravimetrically calibrated by the manufacturer but was
207 not used at the calibration temperature requiring the output to be calibrated by a Tekran 2537B. After the
208 equipment was moved to the RAMIX site the permeation tube output increased. The authors also
209 acknowledge a significant uncertainty ($\pm 15\%$) in the RAMIX manifold flow measurements that were
210 required to calculate spike concentrations; hence this is the minimum uncertainty in calculated spike
211 concentrations.

212 In fact, we find that several independent measurements of Hg(0) spikes differ by as much as 30%
213 from the value calculated by the manifold operators suggesting that ($\pm 15\%$) underestimates the
214 uncertainty. Because of these considerations we believe the RAMIX manifold is best treated as a semi-
215 quantitative delivery system that was not well characterized. We do not feel it is appropriate to characterize
216 “recoveries” as Gustin et al. (2013) have done because of the large uncertainty in Hg(0) spike
217 concentrations. Rather, it is most useful to focus on sampling periods when multiple independent
218 instruments show reasonable agreement.

219

220 3.2 UM Tekran Performance

221 In evaluating the first week of the UM RAMIX measurements it became clear that there was some non-
222 linearity in the relative responses of the 2P-LIF and UM Tekran systems and that better agreement was
223 obtained by referencing the Hg(0) concentration to the UNR Tekran. Gustin et al., (2013) concluded that
224 the UNR Tekran, based on the inlet configuration, only measured Hg(0) and they suggested that the UM
225 system, due to the long sampling line, was measuring total gaseous mercury (TGM). We compared the
226 manifold Hg(0) readings from the UM and UNR Tekrans over the first 260 hours in which we took
227 measurements. The absolute concentration difference relative to the UNR instrument is shown in Figure 1.
228 Hour zero corresponds to 9 am on August 26th when we started measurements and hour 260 corresponds to
229 midnight on September 5th. Over the first 24 hours the UM Tekran is offset by $\sim 0.5 \text{ ng m}^{-3}$ and the offset
230 jumps to $\sim 2 \text{ ng m}^{-3}$ at hour 30 on August 27th with the difference decreasing over the next week of
231 measurements in an almost linear fashion. Over most of this period the UW Tekran did not report Hg(0)
232 measurements other than a small set of measurements on August 28th that are offset by $\sim 0.5 \text{ ng m}^{-3}$ relative
233 to the UNR Tekran. It can be seen that by hour 250 on September 5th all three instruments had converged.
234 After this period the agreement between the UW, UNR and UM Tekrans was good until September 8th,
235 when the UM instrument became contaminated after a malfunction of our external permeation oven,
236 requiring replacement with a backup Tekran 2537A unit. Both the absolute response and the response
237 factor, i.e. the calibration factor of the UM Tekran were somewhat unstable during this period and
238 additional details are provided in the Supplementary Information. Our focus during this initial period of the
239 intercomparison was on the two laser systems that were being set up. In retrospect we can acknowledge
240 that greater attention should have been paid to quality assurance with the UM Tekran. We conclude that the
241 difference between the UM and UNR instruments is an experimental artifact. Problems with instability in
242 the UM Tekran may have been associated with the use of an external pump to supplement the internal
243 Tekran pump, or with the fact that the UM instrument had been powered down for almost one week and
244 relocated to a site at a significantly different ambient pressure. It is also noteworthy that the initial abrupt
245 change to a large offset followed by the offsets shown in Fig. 1 occurred prior to the start of the manifold
246 spikes of HgBr₂ and cannot be associated with the elevated levels of HgBr₂ that were introduced into the
247 manifold on Sept. 5th. The differences between the instruments cannot, in our view, be indicative of any
248 type of chemistry within our sampling lines, nor can it be indicative of the UM instrument measuring TGM
249 rather than Hg(0).

250

251 **3.3 2P-LIF Measurements**

252 The absolute Hg(0) concentrations reported for the 2P-LIF measurements typically use a single 10-minute
253 section of Tekran concentration data to calibrate the 2P-LIF signal and place it on an absolute concentration
254 scale. The complete time series of measurements then gives a long-term comparison of the 2P-LIF and
255 Tekran instrumentation with the absolute 2P-LIF concentrations based on the single 10-minute calibration
256 point.

257

258 **3.3.1 September 5th**

259 This was the first occasion on which the three independent Tekran 2537 instruments and the 2P-
260 LIF system reported simultaneous measurements. The 2P-LIF system sampled from the RAMIX manifold
261 for approximately 6.5 hours from ~10:30 am to 5 pm. Over the course of the sampling period there were
262 two spikes of Hg(0) lasting one and two hours, respectively. The UW manifold team reported an initial 10
263 am Hg(0) spike concentration of 26.5 ng m⁻³ dropping to 24.4 ng m⁻³ over the course of the one hour spike.
264 The two hour spike that began at 1 pm was reported to be ~12.4 ng m⁻³ dropping to 10.5 ng m⁻³ over the
265 course of two hours. The ambient airflow in the manifold was spiked with HgBr₂ for the whole of this
266 sampling period and the reported level of the HgBr₂ spike varied between 0.6-0.7 ng m⁻³. The levels of
267 HgBr₂ measured by the DOHGS instrument were consistent with this but the concentrations reported by the
268 UNR speciation units were considerably lower and with a significant discrepancy between the two
269 speciation units. Figure 2a shows the sequence of Hg(0) measurements from the UNR, UW and UM
270 Tekrans together with the 5 minute averages of the 2P-LIF signal. The 2P-LIF instrument began manifold
271 measurements in the middle of the initial 10 am Hg(0) spike and is scaled to the concentration at this time
272 which all three Tekrans measured as ~22.5 ng m⁻³. The three Tekrans agree to better than 5% during both
273 of the manifold spikes and, based on a pre-spike ambient concentration of 2 ng m⁻³ it suggests that the
274 initial spike concentration was ~20.5 ng m⁻³. This suggests that the reported spike concentration was ~25-
275 30% larger than the actual concentration introduced into the manifold. Fig. 2b shows an expanded
276 concentration scale to highlight the nominally ambient measurements. There is some suggestion that it took
277 some time for the spike to be completely removed, particularly after the second spike. At the completion of
278 the second spike all the instruments drop to ambient but the UNR instrument sees two Hg(0) “pulses”.
279 Interestingly these show up with greatly reduced amplitudes in the UW and UM Tekran signals and also in
280 the 2P-LIF signal. Figure 3 shows the % difference of the other instruments relative to the UM Tekran and
281 over most of the sampling period the agreement between all the measurements is better than 10% over an ~
282 7 hour period with 5 minute sampling resolution. This indicates that the 2P-LIF instrument is capable of
283 stable operation over an extended time period with any drifts being corrected by normalization to the
284 reference cell. Well calibrated independently operated Tekrans should be capable of agreement to better
285 than 5% based on tests performed by the manufacturer and this level of agreement is achieved during
286 subsets of the sampling period. It is not clear if the deviations that are observed, particularly the large
287 deviations seen by the UNR Tekran after the second spike are related to presence of elevated levels of
288 HgBr₂ or other issues related to manifold operation. The fact that all the instruments observed these Hg(0)
289 pulses suggests that the artifact may be related to a process in the manifold rather than in in the UNR
290 sampling line. However the significant differences in the magnitude of Hg(0) pulses observed by the
291 different instruments are difficult to rationalize.

292

293 **3.3.2 September 1st and 2nd**

294 The UM and UNR systems sampled simultaneously for a 22 hour period offering an opportunity to
295 compare the instruments over an extended sampling period. This sampling also occurred prior to any of the
296 manifold spikes that introduced substantial concentrations of HgBr₂ into the manifold and sampling lines.
297 Unfortunately, the UW instrument did not report any measurements during this sampling period. The UM
298 system sampled for 26 hours and the complete dataset is described elsewhere, (Bauer et al. 2014). This
299 includes a detailed analysis of the short-term, i.e. 1-10 second, variation in the Hg(0) concentration and the
300 ability of the 2P-LIF system to capture this. Here we focus on the simultaneous sampling period and the
301 variability that should be resolvable by both of the Tekrans and the 2P-LIF instruments. SI Figure 1 shows
302 the 24 hour sampling period with the 2P-LIF signal calibrated by the UM Tekran concentration at the
303 beginning of hour 13 (i.e. 1 pm on September 1st) and the corresponding measurements from the UNR
304 Tekran. SI Figure 2 shows the same data with an expanded y-axis to highlight the variation in the ambient
305 measurements. All three instruments track each other quite well over the first 10 hours and then measure a
306 nocturnal increase in Hg(0) which shows greater mid-term variability in the concentration. The 2P-LIF
307 concentrations are approximately 20% greater than the Tekran measurements during this period. At hour 33
308 (i.e. 9 am on September 2nd) there was a manifold spike with a reported concentration of 12.9 ng m⁻³
309 dropping to 11.9 ng m⁻³ over the course of one hour. The UNR Tekran is ~6% lower, the UM Tekran is
310 ~20% lower and the 2P-LIF ~22% higher than the calculated spike concentration. SI Figure 3 shows the
311 same measurement set but with all instruments normalized to the second manifold spike at hour 33. Figure
312 4 shows an expanded y-axis, the concentration scale, focusing on the ambient concentration measurements.
313 It is apparent that we now see better agreement between the 2P-LIF and the UNR Tekran but that the UM
314 Tekran lies systematically higher than the UNR Tekran. Figure 5 shows a three hour subset of the
315 measurements corresponding to 5-8 am on the morning of September 2nd. The variation between the
316 instruments is greater than 5% and the short term variations in the Hg(0) concentration vary between the
317 three instruments. Using either calibration approach we see that all instruments capture both the nocturnal
318 increase in Hg(0) concentration and the greater variability in the signal but that there are differences in the
319 amplitude of the variability.

320

321 3.3.3 Hg(0) Intercomparison Conclusions

322 Almost all of the measurements of atmospheric concentrations of Hg(0) have been made with
323 CVAFS instrumentation and the majority of those measurements have utilized the Tekran 2537. This work
324 provides the first extensive comparison of the Tekran 2537 with an instrument that is capable of fast in-situ
325 detection of Hg(0) using a completely different measurement technique. Measurements over two extended
326 sampling periods show substantial agreement between the 2P-LIF and Tekran measurements and suggest
327 that all the instruments are primarily measuring the same species. Intercomparison precision of better than
328 25% was achievable over an extended sampling period and precision of better than 10% was achieved for
329 subsets of the sampling period. As we discuss below it is difficult to determine the extent to which
330 interferences from RGM contribute to the differences observed.

331

332 **3.4 Interference Tests.**

333 As noted above, one component of the initial RAMIX proposal was an examination of the response of the
334 various sensors to potential interfering compounds HgBr₂, O₃ and H₂O. An analysis of the 2P-LIF
335 detection approach suggests that at the spike levels employed during the RAMIX campaign, neither HgBr₂
336 nor O₃ should have any interference effects. Changes in the concentration of H₂O do affect the 2P-LIF
337 signal because H₂O absorbs the 2P-LIF fluorescence signal and may quench the fluorescence. In addition,
338 O₂ also absorbs the 2P-LIF signal and quenches fluorescence thus a change in the O₂ concentration will
339 affect the linearity of the response. We have presented a detailed discussion of these effects (Bauer et al.,
340 2014) including an examination of two types of interferences that have been observed in LIF sensors
341 applied in atmospheric and combustion environments and concluded that these are not potential problems
342 in 2P-LIF measurements of atmospheric Hg(0). As we have noted previously (Bauer et al., 2014),
343 condensation in our sampling lines can produce artifacts in Hg(0) concentration measurements. Because of
344 the low humidity in Reno it was not necessary to use any type of cold trap during ambient measurements
345 but we did use a trap during manifold spikes of H₂O so our measurements do not address this as a potential
346 interference.

347 **3.4.1 O₃ Interference Tests.**

348 On September 7th an ozone interference test was conducted by simultaneously spiking the
349 sampling manifold with high concentrations of Hg(0) and ozone. The spike in Hg(0) lasted from 9am to
350 7:30 pm and there were two ozone spikes, each two hours in duration. A comparison of the UM, UW and
351 UNR Tekrans and the 2P-LIF signal is shown in Figure 6. The UW Tekran only measured for a portion of
352 this period but agrees reasonably well with the other Tekrans. The 2P-LF signal is calibrated by the UM
353 Tekran reading during the initial Hg(0) spike at hour 9.30. The 2P-LIF signal was online for 6 minutes at
354 the beginning of the first ozone spike and then went offline for ~40 minutes for instrument adjustments.
355 When the 2P-LIF came back online the magnitude of the normalized signal was low relative to the Tekrans.
356 At hour 13 all three instruments converge and agree well over the course of the second spike. The
357 magnitude of the 2P-LIF signal could have been affected adversely by the adjustments but any reduction in
358 signal should have been compensated by a corresponding change in the reference cell. The elevated levels
359 of ozone were introduced into the manifold by UV irradiation of O₂ and adding the O₂/O₃ gas mixture
360 directly into the manifold produced a reported ~8% relative increase of O₂ levels in the manifold mixing
361 ratio. As we note above, this additional O₂ would absorb some of the 2P-LIF signal but this would be a
362 very small effect. The enhanced quenching by O₂ is more difficult to assess but cannot explain the
363 discrepancy between the Tekrans and the 2P-LIF signal. In addition the agreement during the second ozone
364 spike was good. One possible explanation is that the increase in the O₂ mixing ratio was larger than
365 calculated for the first spike. A second series of O₃ spikes were conducted on September 13th when we were
366 attempting to measure total mercury using pyrolysis as described below. The 2P-LIF measurements
367 switched on a five-minute cycle between a pyrolyzed line that would have decomposed all the ozone in the

368 sample and a line containing the ambient air spiked with ozone. There was no difference in the 2P-LIF
369 signal from the two sampling channels again suggesting that O₃ has no interference effects.

370 The changes in the Hg(0) concentration measurements shown in Figure 6 track the predicted
371 changes in calculated spike concentration. However the calculated spike concentrations, which are also
372 shown, are 20-40% higher than the actual measurements made by the Tekrans.

373

374 **3.5 Measurements of TM and TOM**

375 We made attempts to use the 2P-LIF instrument to measure TM and hence TOM by difference by sampling
376 through two manifold lines. A pyrolyzer was located at the manifold on one of the sampling lines to
377 measure TM. The other sampling line measured ambient Hg(0). TOM was calculated from the difference in
378 the TM and Hg(0) concentrations and in this sampling configuration the limit of detection for TOM
379 depends on the short term variability in ambient Hg(0) which is significant and shows a diurnal variation.
380 The pyrolysis system was set up and tested on September 12. Manifold sampling was conducted on the 13th
381 and 14th and sampling from the trailer roof occurred on the 15th. We calculated the means of the pyrolysis
382 and ambient channel concentrations and the difference which gives the TOM concentration. We also
383 calculated the standard deviations and standard errors (SE) and used these errors to calculate in quadrature
384 the 2SE uncertainty in the derived TOM concentration. However, as discussed below, the errors in the
385 means do not appear to capture the full variability in Hg(0), particularly at shorter sampling times.

386 **3.5.1 September 14th**

387 Our most extensive sampling took place on the 14th when we were able to sample for three ~ 2 hour periods
388 between 9 am and 8 pm. On this day, there were multiple manifold spikes of HgBr₂ and also an Hg(0) spike
389 and we have made a detailed analysis of the data for each sampling period.

390 The third sampling period which included a large HgBr₂ spike provided the only definitive
391 opportunity to demonstrate the capability of 2P-LIF coupled with pyrolysis to measure oxidized mercury.
392 The third sampling period began at ~ hour 17.3 during a manifold HgBr₂ spike that began at hour 17. A
393 short Hg(0) spike was also introduced at hour 18. Fig. 7 shows the 2P-LIF signals from the ambient and
394 pyrolyzed sampling lines together with the means and 1 standard deviation. The UM Tekran was offline at
395 this time and so the 2P-LIF concentrations are calibrated by the concentrations reported by the UNR
396 Tekran at the beginning of the Hg(0) spike which are also shown. Both the UNR Tekran and UW Tekran
397 report very similar Hg(0) concentrations during the Hg(0) spike. Both systems report an Hg(0)
398 concentration of 6.7 ng m⁻³ at the beginning of the spike which, since the pre-spike concentration was ~1.9
399 ng m⁻³, corresponds to a spike concentration of 4.8 ng m⁻³. This is lower than the calculated spike
400 concentration of 6.1 ng m⁻³ reported by the manifold operators and suggests that the calculated spike was
401 ~27% higher than the actual spike concentration introduced into the manifold. Fig. 8 shows the means of
402 each set of ambient and pyrolyzed measurements together with the 2σ variation and 2SE of the mean. Fig. 9
403 shows the TOM concentrations calculated from the difference together with 2SE in the TOM concentration.
404 The reported spike concentrations and DOHGS measurements are also shown. During the initial sampling

405 period between ~17.3- 17.8 hours the 2P-LIF pyrolysis measurements do not show evidence for an HgBr₂
406 spike. Taking the difference between the ambient and pyrolyzed measurements during this period we obtain
407 [TOM] = 0.05±0.05 ng m⁻³. Shortly before the introduction of the Hg(0) spike we see clear evidence for an
408 increase in the Hg(0) concentration in the pyrolysis sample relative to the ambient sample. We speculate
409 that the manifold adjustments that were made to introduce the additional Hg(0) spike produced either a
410 change in the flow or some other change in the manifold conditions that allowed the HgBr₂ spike to reach
411 our pyrolyzer, which, as mentioned above, was located at the manifold. This difference between the two
412 2P-LIF signals is clearly evident by inspection of Fig.7. Fig. 9 shows that the TOM concentration which
413 should consist almost exclusively of HgBr₂ is significantly larger than both the reported HgBr₂ spike
414 concentration and the concentrations reported by the DOHGS system which are in perfect agreement.
415 Taking the difference between the ambient and pyrolyzed measurements for hour 18.02-18.35 we obtain
416 [TOM] = 1.20±0.17 ng m⁻³ with 2SE uncertainty. It is important to note again that the calculated Hg(0)
417 spike concentration is 27% larger than the measured concentration. This large difference is most likely due
418 to errors in the flows or the permeation source output but it suggests that little confidence can be placed in
419 the calculated concentration of the HgBr₂ spike. In addition, it is clear that the DOHGS measurements
420 show a different temporal profile of TOM. The DOHGS system reports TOM concentrations that agree
421 almost exactly with the calculated spike concentration at the beginning of the spike period and drop to a
422 very low background level that is below the detection limit at the end of the reported spike period. In
423 contrast, the 2P-LIF measurements do not show an increased TOM concentration until shortly before the
424 introduction of the Hg(0) spike and they take ~20 minutes to drop to background levels. The UNR
425 speciation systems sample for 1 hour and this is followed by a 1 hour analysis period so they produce a
426 single hourly average every two hours. During this period the UNR speciation system Spec1 sampled for ~
427 20 minutes during the spike period and then for a further 40 minutes. Spec2 was sampling ambient air
428 outside the manifold.

429 SI Fig. 4 shows the 7s average of the 2P-LIF signal from the ambient and pyrolysis sample lines
430 for the first sampling period at hours 8-10.45 together with the mean and 1 standard deviation (1σ)
431 variation in the 2P-LIF signals. SI Fig. 5 shows the means together with the 2σ variation and 2SE of the
432 mean. It is clear that there is significant short term variability in the ambient Hg(0) concentration. SI Fig. 6
433 shows the TOM concentrations calculated from the difference between the pyrolyzed and ambient channels
434 together with the calculated 2SE in the TOM concentration. The reported spike concentration is also
435 shown. If we take the means of the 2P-LIF ambient and pyrolysis measurements during the reported spike
436 period we obtain: ambient: 2.06±0.05 ng m⁻³ and pyrolyzed: 2.21±0.03 ng m⁻³ giving a TOM concentration
437 of 0.145±0.05 ng m⁻³. The 2P-LIF measurements are consistent with the detection of TOM but they are
438 much lower than the calculated spike and DOHGS measurements shown in Fig. 10.

439 SI Figs.7-9 show the corresponding plots for the second sampling period from ~ 12.2-14 hours.
440 The alternating sampling between the ambient and pyrolysis channels is more even and SI Fig. 7 shows that
441 there is still variability in ambient Hg(0). The means of all the samples give: ambient: 1.72±0.02 ng m⁻³,

442 pyrolyzed: $1.70 \pm 0.02 \text{ ng m}^{-3}$. If we take the subset of measurements that coincide with the reported spike
443 we obtain: ambient: $1.79 \pm 0.02 \text{ ng m}^{-3}$ pyrolyzed $1.77 \pm 0.02 \text{ ng m}^{-3}$. In this case, the 2P-LIF measurements
444 do not detect HgBr_2 and are not consistent with the reported spike or DOHGS measurements.

445 SI Figs. 10 and 11 show the averages of the TOM concentrations from the 2P-LIF system together
446 with the measurements from the UNR speciation systems, the reported spike concentrations and 5 min
447 DOHGS concentrations. During this sampling period Spec1 sampled from the RAMIX manifold while
448 Spec2 sampled ambient air outside the manifold. Gustin et al. (2013) detail problems with the response of
449 the Spec2 system and applied a 70% correction that is also shown as “Spec2 corrected”. Because both the
450 DOHGS and 2P-LIF pyrolysis systems are expected to measure the sum of gaseous (RGM) and particulate
451 (PBM) oxidized mercury we have plotted the sum of the RGM and PBM concentrations from the
452 speciation systems. They are plotted at the mid-point of the 1 hour sampling period.

453 Over most of the measurement period the 2P-LIF pyrolysis and Spec1 measurements are
454 consistent and lower than the DOHGS measurements. The exception is the large spike in TOM seen by the
455 2P-LIF system at hour 18. The spike occurred during the initial portion of Spec1 sampling and, although it
456 measures an increase in RGM relative to Spec2, the magnitude is not consistent with the 2P-LIF pyrolysis
457 observations.

458 3.5.2 September 13th

459 September 13th was the first day we were able to sample with the pyrolysis system and we sampled over a
460 period of 5 hours. The only manifold spike during this period was an O_3 spike at 1 pm that lasted one hour,
461 so the speciation instruments were attempting to measure ambient RGM. SI Fig. 12 shows averages of
462 TOM concentrations as measured by the 2P-LIF pyrolysis system together with the hourly averages as
463 measured by the DOHGS and UNR speciation instruments. The x-axis error shows the duration of the 2P-
464 LIF measurements together with 2SE y-axis error bars. Two of the averages of the 2P-LIF measurement
465 give a physically unrealistic negative concentration suggesting that combining the 2SE errors in the means
466 of the ambient and pyrolyzed channels underestimates the uncertainty in the TOM measurement.

467 3.5.3 September 15th

468 On September 15th we sampled from the trailer roof using the same sampling lines and again
469 alternating between the pyrolyzed and unpyrolyzed channels. SI Fig. 13 shows the averages of the 2P-LIF
470 signal from the ambient and pyrolysis channels together with the concentrations measured by the Spec2
471 system that was sampling ambient air outside the manifold. The concentration obtained from the UM
472 denuder samples described below are also shown. The UW DOHGS and Spec1 systems were sampling
473 from the RAMIX manifold with continuous HgBr_2 spiking during this period. We see some evidence for
474 measurable RGM in the first hour of the measurements and this is not seen by Spec 2. Later measurements
475 show no evidence for measurable RGM concentrations.

476

477 3.6 Limits of 2P-LIF detection of TOM

478 As we have noted above, our limit of detection of TOM depends on the short term variability in
479 the ambient Hg(0) concentration because we use a single fluorescence cell and switch between pyrolysis
480 and ambient channels. We have attempted to give an estimate of the uncertainty by taking two standard
481 errors of the means and combining the errors in quadrature to get an estimate of the uncertainty in the TOM
482 concentration. If the mean of the ambient Hg(0) concentration is not fluctuating significantly on the
483 timescale of channel switching this approach should give an accurate estimate of the uncertainty in TOM.
484 In fact, our Hg(0) observations show that the fluctuations in the Hg(0) concentration show a significant
485 diurnal variation, with large fluctuations at night, decreasing over the course of morning hours and being
486 smallest in the afternoon. This can be seen in the long term sampling from September 1st and 2nd and in the
487 observations from September 14th. The observation of statistically significant but physically unrealistic
488 negative TOM concentrations on September 13th may be explained by this. Such an artifact could be
489 produced by contamination in the Teflon valve switching system that alternates the flow to the fluorescence
490 cell. This type of contamination should produce a constant bias that is not actually observed. It appears that
491 the short term variability in Hg(0) concentration produces a small bias in some cases that is not averaged
492 out by switching between the ambient and pyrolyzed channels. For example, on September 13th the initial
493 sample period of 1.2 hours gives an RGM concentration of $0.06 \pm 0.10 \text{ ng m}^{-3}$ while two shorter sampling
494 periods at hour 10.5 (36 min sample) and 13.5 (12 min sample) give $0.15 \pm 0.09 \text{ ng m}^{-3}$. Our results suggest
495 that the use of a single detection channel with switching between ambient and pyrolyzed samples is not
496 adequate to resolve the small concentration differences that are necessary to be able to monitor ambient
497 TOM. It is essential to set up two detection systems, one continuously monitoring ambient Hg(0) and the
498 other continuously monitoring a pyrolyzed sample stream giving TM, to get the precision needed to
499 monitor ambient TOM. Over most of the measurement periods our results are consistent with the lower
500 TOM values reported by the UNR speciation instruments although there is a large uncertainty in the
501 concentrations that is actually difficult to quantify. In addition, it is important to emphasize that this was
502 our first attempt to use the pyrolysis approach to attempt to measure TOM. It is possible that the pyrolyzer
503 was not working efficiently on September 13th. The results from September 14th are more difficult to
504 rationalize. The 2P-LIF pyrolysis system has the sensitivity to detect the much higher values of RGM
505 reported by the DOHGS system and the reported spike concentrations of HgBr₂. At higher concentrations,
506 as shown in Fig. 9, the 2P-LIF system can monitor HgBr₂ with ~10 minute time resolution. Our results,
507 however, cannot be reconciled with those reported by the DOHGS system or the spike concentrations
508 reported by the UW manifold team.

509

510 **3.7 Manual Denuder Measurements:**

511 As we describe above, our use of manual denuders was similar to that described by Landis et al. (2002)
512 with the exception that we did not incorporate the integrated elutriator/acceleration jet and impactor/coupler
513 on the denuder inlet and the denuders were not heated. Landis et al. (2002) suggest that HgCl₂ is
514 quantitatively transported through the manual denuder elutriator/impactor inlet when properly heated. In

515 later work, Feng et al. (2003) reported that such impactors could reduce the efficiency of RGM collection
516 although in that work there is no reference to the temperature of the impactor. In this work, no type of
517 particle filtering was used on the inlets. In addition, we used single photon LIF to monitor the evolution of
518 Hg(0) in real-time as the RGM decomposed on the hot denuder surface during oven analysis. The analysis
519 was carried out in He buffer gas and the Hg(0) concentration was calibrated by manual injections. The first
520 series of measurements, i.e. September 6-14th involved single denuder sampling. On the 15 and 16th we
521 employed tandem sampling with two denuders in series to assess the extent of RGM “bleedthrough”. We
522 used two sets of denuders on the 15th and four sets of denuders on the 16th. Fig. 10 shows the raw data for a
523 denuder analysis showing the preheat Hg(0) calibration injections and the temporal profile of the Hg(0) LIF
524 signal for one of the September 16th samples, denuder 1. The two traces correspond to the two monitoring
525 PMTs set at different gains to increase the dynamic range of the measurements. Fig. 11 shows the
526 calibrated profile for the same denuder together with the “blank” i.e. the trailing denuder. The complete set
527 of manual denuder data together with corresponding values for the UNR speciation units that are closest in
528 sampling time are shown in Table 1. Sampling occurred on denuders 1, 4, 6 and 7. The “trailing” denuders
529 which we have treated as blanks are denuders 3, 5, 8 and 9. The advantage of monitoring the RGM
530 decomposition in real-time is shown in the September 16th data. The temporal decomposition profiles
531 (TDP) for three of the denuders shown in Fig. 11 and SI Figs 14 and 15 show reasonable agreement both in
532 absolute concentration of Hg(0) and the time for decomposition to occur. The fourth denuder sample, SI
533 Fig. 16, is a factor of 4-5 higher in concentration and decomposes on a longer time scale with significant
534 structure in the TDP. Comparing the TDPs for all eight denuders it is clear that the TDP for denuder 7,
535 which shows the anomalously high value, is very different from the TPDs for the other three sample
536 denuders. We believe that this TDP is associated with particulate mercury that has impacted on the denuder
537 wall and decomposes on a slower timescale giving a very different temporal profile from RGM that was
538 deposited on the denuder wall. SI Table 1 shows the values of RGM obtained from denuder analysis
539 together with an indication of impact from a PBM component. We have also included measurements from
540 the UNR speciation systems that overlap with, or are close to, the times when our measurements were
541 made. We draw several conclusions from the measurements. The values we obtain from simultaneous
542 measurements that are not influenced by the presence of PBM agree reasonably well with each other, are
543 broadly consistent with the values reported by the Tekran speciation systems and are typically much lower
544 than the values from the UW DOHGS system. Two sets of tandem denuder measurements from September
545 15 and 16 indicate that there is not a significant level of “bleedthrough” onto the trailing denuders. This
546 suggests that the large differences between the DOHGS system and the UNR speciation systems are not
547 due to specific problems with the RAMIX manifold or the speciation systems deployed at RAMIX even
548 though Spec 2 was not functioning properly as documented by Gustin et al. (2013). The tandem sampling
549 also demonstrates that any denuder artifact is not a result of some type of “bleedthrough” artifact that is
550 preventing RGM from being quantitatively captured by the first denuder. These results are consistent with
551 prior work by Landis et al. (2002) and Feng et al. (2003). It is also noteworthy that the manually sampled

552 denuders were at ambient temperature in contrast to the speciation denuders that are held at 50 C. Hence
553 the absolute sampling humidities are similar but the relative humidities are very different. Finally, we
554 suggest that there is value in monitoring RGM decomposition in real time as diagnostic of particulate
555 impact when utilizing the annular denuders without the impactor inlet designed to remove coarse
556 particulate matter that may be retained due to gravitational settling

558 **4.0 Implications of RAMIX results.**

559 We think a realistic assessment of the RAMIX results is imperative because the interpretation of
560 the RAMIX data and the conclusions presented by Gustin et al. (2013) and Ambrose et al. (2013) have
561 enormous implications for both our understanding of current experimental approaches to atmospheric
562 sampling of mercury species and for the chemistry itself. Speciation systems using KCl denuder sampling
563 are widely used in mercury monitoring networks worldwide to measure RGM concentrations and the
564 Gustin et al. (2013) and Ambrose et al. (2013) papers suggest these results greatly underestimate RGM
565 concentrations with no clear way to assess the degree of bias.

566 **4.1 Intercomparison of Hg(0)**

567 The assessment of the Hg(0) measurements is a little different in the two manuscripts with
568 Ambrose et al. (2013), noting that “comparisons between the DOHGS and participating Hg instruments
569 demonstrate good agreement for GEM” where GEM refers to Hg(0), and they found a mean spike recovery
570 of 86% for the DOHGS measurements of Hg(0), based on comparisons between measured and calculated
571 spike concentrations. Gustin et al. (2013) suggest that the UM Tekran agreed well with measurements of
572 TM reported by the DOHGS system and they “hypothesize that the long exposed Teflon line connected to
573 the UM Tekran unit provided a setting that promoted conversion of RM to GEM, or that RM was
574 transported efficiently through this line and quantified by the Tekran system. The latter seems unlikely
575 given the system configuration...”, where RM refers to reactive mercury. As we note above, we believe
576 that the best explanation for discrepancies between the UM and UNR Tekrans is an experimental issue with
577 the UM Tekran response during the initial period of sampling. We would suggest that data from September
578 5th, one of the few occasions when data from multiple instruments agreed over an extended period is not
579 compatible with either transmission or inline reduction of RGM in our sampling line. What is also
580 significant from this data is the very large discrepancy between the spike concentrations as measured
581 independently by three different Tekran systems and confirmed by the relative response of the 2P-LIF
582 measurements and the calculated spike concentration. The discrepancy, on the order of 25-30%, is larger
583 than the manifold uncertainties suggested by Finley et al. (2013). We note other examples of the measured
584 Hg(0) spikes being significantly lower than the calculated concentrations. In prior work we have shown
585 that both the Tekran and 2P-LIF systems show excellent agreement over more than 3 orders of magnitude
586 in concentration when monitoring the variation in Hg(0) in an N₂ diluent. It is to be expected therefore that
587 the “recovery” of high concentration spikes should show good agreement between the different instruments
588 as observed in the September 5th data. The difference between the observations and the calculated manifold

589 spike concentrations is, we would suggest, a reflection of the significant uncertainty in the calculated
590 manifold spike concentration and is not a reflection of reactive chemistry removing Hg(0). In addition,
591 random uncertainties in the flow calculations should not produce a consistently low bias relative to the
592 calculated spike concentrations. As we note above in section 3.1, Ambrose et al. report an increase in the
593 output of their Hg(0) permeation tube after the move to the RAMIX site but this assumes that their Tekran
594 calibration is accurate. The results are consistent with their Tekran measuring too high an output from the
595 permeation device. This is significant if the same Tekran is being used to calibrate the output of the HgBr₂.

596 A more difficult issue is the question of resolving the differences in the temporal variation of
597 ambient Hg(0) at the 5 minute timescale as captured by the different instruments. The Tekran systems
598 should be in agreement with a precision of better than 5% and the 2P-LIF system, with a much faster
599 temporal resolution and detection limit, should be capable of matching this. The differences here are not
600 consistently associated with a single instrument with, for example, the 2P-LIF having some systematic
601 offset with respect to the CVAFS systems. The extent to which the larger (i.e. larger than 5%) observed
602 discrepancy which ranged from 10% to 25% is a result of interferences or simply a reflection of instrument
603 precision is difficult to assess. We note again that the UM instruments had to sample through a very long
604 sampling line and we expect that oxidized mercury is deposited on the sampling line. However it is not
605 possible to assess the extent to which oxidized mercury is reduced back to its elemental form introducing
606 small artifacts. As we suggest below, an intercomparison of instrument response to variation in Hg(0)
607 concentrations in a pure N₂ diluent with the Hg(0) concentration varying between 1-3 ng m⁻³ would provide
608 a definitive baseline measurement of the instrument intercomparison precision and accuracy. We suggest
609 that such a measurement is a critical component of any future intercomparison of mercury instrumentation.

610

611 **4.2 Comparison of Total Oxidized Mercury**

612 To the best of our knowledge, RAMIX is the only experiment that has measured ambient TOM using
613 multiple independent techniques. It should again be emphasized that the TOM measurements using
614 pyrolysis with 2P-LIF detection were the first attempt to perform such measurements and the use of a
615 single channel detection system introduced large uncertainties into the measurements. The very large
616 discrepancies between the measurements of TOM reported by the DOHGS system, the Tekran speciation
617 systems and the limited number of 2P-LIF pyrolyzer measurements are the most problematic aspect of the
618 RAMIX measurement suite. Work prior to RAMIX suggested a potential ozone and/or humidity
619 interference in the operation of KCl coated annular denuders and a number of studies since have also
620 reported such an effect (Lyman et al., 2010; McClure et al., 2014). Typically however, the differences
621 between the RAMIX measurements are large and are not germane to the differences between the DOHGS
622 and 2P-LIF pyrolyzer measurements. The SI Figures give an example of the differences between the
623 DOHGS measurements and the denuder and 2P-LIF measurements. Ambose et al. (2013) note that the
624 DOHGS measurements were, on average, 3.5 times larger than those reported by the Spec1 system and
625 summarize the comparison with denuder measurements as follows: “These comparisons demonstrate that

626 the DOHGS instrument usually measured RM concentrations that were much higher than, and weakly
627 correlated with those measured by the Tekran Hg speciation systems, both in ambient air and during HgBr₂
628 spiking tests.” The discrepancy of a factor of 3.5 is an average value but, for example, examining the
629 September 14 data at ~5 am the DOHGS system is measuring in excess of 500 pg m⁻³ compared with ~20
630 pg m⁻³ measured by the speciation systems, a factor of 25 difference. At this point, the Hg(0) concentration
631 was ~3 ng m⁻³ so based on the DOHGS measurements oxidized mercury is ~15% of the total mercury
632 concentration. A recent study by McClure et al. (2014) provided a quantitative assessment of the extent to
633 which ozone and humidity impact the recovery of HgBr₂ on KCl recovery. They note that although they
634 provide a recovery equation to compare with other studies, they do not recommend use of this equation to
635 correct ambient data until more calibration results become available. In Fig. 12, we show the ozone
636 concentration and absolute humidity for a 35 hour sampling period on September 13th and 14th that included
637 two ozone spikes and only sampled ambient TOM. Fig. 13 shows the expected denuder recovery based on
638 the formula determined by McClure et al. which varies between a typical value of ~70% dropping to ~50%
639 during the ozone spikes. The figure also shows the reported recoveries, i.e. the ratio of RGM as measured
640 by either the UNR speciation systems or the 2P-LIF system divided by the value reported by the DOHGS
641 system. These values are typically much lower than those predicted by the McClure recovery expression. In
642 addition, on September 13th and for most of the 14th, the 2P-LIF pyrolysis system sees little or no evidence
643 for high spike concentrations of HgBr₂ but records levels that fluctuate around those reported by the
644 speciation systems. The one exception is the spike at hour 18 on September 14th.

645 We suggest that the ability of the 2P-LIF pyrolysis system to monitor large spike concentrations is
646 shown by the measurements during the September 14th HgBr₂ spike at hour 18. The evidence for an
647 enhancement in the pyrolyzed sample stream is observable in the raw 7s averaged data and becomes clear
648 taking 5 minute averages. The absolute value of the pyrolyzed enhancement is obtained relative to the
649 concentration of the Hg(0) during the spike taken from the measurements by the UNR Tekran that are in
650 excellent agreement with the DOHGS Hg(0) values. The 2P-LIF measurements show a significantly larger
651 HgBr₂ concentration and a different temporal profile compared with the DOHGS instrument. In particular,
652 it is very difficult to rationalize the difference between the 2P-LIF and DOHGS systems during the first
653 hour of the spike. We would suggest it is difficult to make the case that both instruments are measuring the
654 same species. It is clear that the 2P-LIF pyrolyzer is operating efficiently based on the clear observation of
655 TOM at the end of the spike. We again note that the 2P-LIF system is not sensitive to TOM. It is important
656 to note that the DOHGS instrument requires an inline RGM scrubber to remove RGM before the
657 measurement of Hg(0). This inline scrubber utilizes deposition on uncoated quartz wool and the results of
658 Ambrose et al. (2013) imply that while uncoated quartz captures RGM efficiently in the presence of O₃,
659 quartz with a KCl coating promotes efficient reduction to Hg(0).

660 It is also reasonable to question the extent to which the Tekran speciation systems operated at
661 RAMIX reflect the performance of these systems when normally operated under recommended protocols.
662 As noted above, the operation of the RAMIX manifold and the Tekran speciation systems has been

663 questioned by Prestbo (2014). In our view the two most significant issues are the performance of the two
664 2537 mercury analyzers associated with each speciation system and the reduced sampling rate. The
665 performance of the two 2537 units is detailed in Gustin et al. (2013) and, as they noted, there was a
666 significant response in each instrument. Examination of Fig. SI 6 of Gustin et al. (2013) shows the relative
667 responses of the two instruments and using concentrations up to 25 ng m^{-3} , i.e. manifold spikes, they list a
668 regression of $0.72[\text{Hg}(0)] + 0.08$ whereas for the non-spike data they obtain $0.62[\text{Hg}(0)] + 0.25$. Their
669 Table SI 5 lists the regression including spikes as $0.7 (\pm 0.01) + 0.2$, with all concentrations expressed in ng
670 m^{-3} . When considering the use of these analyzers to monitor oxidized mercury the important factor to
671 consider is the loading on the gold cartridge. Their Table SI 3 lists the mean RGM concentrations from
672 manifold sampling as 52 pg m^{-3} for Spec1 and 56 pg m^{-3} for Spec2. For a 1 hour sample at 4 L min^{-1} this
673 corresponds to a cartridge loading of 13 pg. This is similar to the cartridge loading for sampling a
674 concentration of 0.6 ng m^{-3} at 4 L min^{-1} for 5 minutes. If we examine Fig. SI 6 of Gustin et al. (2013) we
675 see that the regression analyses are based on concentrations higher than 0.6 ng m^{-3} , i.e. higher cartridge
676 loadings. At concentrations of 0.6 ng m^{-3} the ratio of Spec2:Spec1 obtained from these regressions would
677 be 1.05, 0.85 and 1.06 depending on which regression formula is used. We should note that based on Table
678 SI 6 of Gustin et al. (2013), the median RGM concentrations in manifold sampling were 41 and 46 pg m^{-3} .
679 The RGM concentrations for free standing sampling were even lower with means of 26 and 19 pg m^{-3} and
680 medians of 23 and 14 pg m^{-3} for Spec1 and Spec2 respectively. For concentrations below 40 pg m^{-3} the
681 cartridge loading drops below 10 pg and in addition, the Tekran 2537 integration routine becomes
682 significant. Swartzendruber et al. (2009) reported issues with the standard integration routine and note that
683 below cartridge loadings of 10 pg the internal integration routine produces a low bias in the $\text{Hg}(0)$
684 concentration. They recommend downloading the raw data, i.e. PMT output, and integrating offline. This
685 issue has recently been discussed by Slemr et al. (2016) in a reanalysis of data from the CARIBIC program.
686 This compounds the problem of correcting the bias between Spec1 and Spec2. Because the speciation
687 instruments were sampling at 4 L min^{-1} rather than the recommended 10 L min^{-1} a large number of the
688 measurements made by the speciation systems are based on uncorrected cartridge loadings of less than 10
689 pg m^{-3} . Based on the above, we caution against drawing significant conclusions based on differences
690 between Spec1 and the corrected Spec2. These differences are the basis of the conclusions of Gustin et al.
691 (2013) that “On the basis of collective assessment of the data, we hypothesize that reactions forming RM
692 (reactive mercury) were occurring in the manifold” (Gustin et al. (2013) abstract). Later they state “The
693 same two denuders, coated by the same operator, were used from Sept 2 to 13, and these were switched
694 between instruments on September 9. Prior to switching the slope for the equation comparing GOM as
695 measured by Spec 1 versus Spec 2 adjusted was 1.7 ($r^2=0.57$, $p<0.5$, $n=76$) after switching this was 1.2
696 ($r^2=0.62$, $p<0.05$, $n=42$). This indicates that although there may have been some systematic bias between
697 denuders Spec2 adjusted consistently measured more GOM than Spec1. We hypothesize that this trend is
698 due to production of RM in the manifold (discussed later).” If reactions in the manifold were producing
699 RM then this production would surely have resulted in the DOHGS measuring artificially high, i.e. higher

700 than ambient, concentrations of oxidized mercury. However, the paper by Ambrose et al. (2013) (written by
701 a subset of the authors of Gustin et al. (2013)) makes no mention of manifold production of oxidized
702 mercury. In fact, Ambrose et al. (2013) state in the supplementary information to their paper, “The same two
703 denuders, prepared by the same operator, were used in the Tekran® Hg speciation systems from 2 to 13
704 September. The denuders were switched between Spec. 1 and Spec. 2 on 9 September. From 2 to 9
705 September, the Spec. 1-GOM/Spec. 2-GOM linear regression slope was 1.7 ($r^2 = 0.57$; $p < 0.05$; $n = 76$);
706 from 9 to 13 September the Spec. 1-GOM/Spec. 2-GOM slope was 1.2 ($r^2 = 0.62$; $p < 0.05$; $n = 42$). These
707 results suggest that the precisions of the GOM measurements made with Spec. 1 and Spec. 2 were limited
708 largely by inconsistent denuder performance.”

709 The oxidized mercury concentrations presented by Ambrose et al. (2013) for the RAMIX
710 measurements suggest a well-defined diurnal profile that peaks at night. It is important to note that the error
711 bars on this profile (Figure 3 of Ambrose et al.) are one standard error rather than one standard deviation.
712 The standard deviations, which actually give an indication of the range of concentrations measured show
713 much larger errors indicating significant day to day variation in these profiles. Nevertheless, the
714 measurements show much larger oxidized mercury concentrations than the speciation systems and the very
715 limited number of 2P-LIF measurements. As we note below, there is no known or hypothesized chemistry
716 that can reasonably explain the large RGM concentrations seen by the DOHGS instrument. Both Gustin et
717 al. (2013) and Ambrose et al. (2013) draw some conclusions about the chemistry of mercury that have
718 significant implications for atmospheric cycling. Gustin et al. suggest in their abstract that “On the basis of
719 collective assessment of the data, we hypothesize that reactions forming RM were occurring in the
720 manifold.” Later in a section on “Implications” they conclude “The lack of recovery of the HgBr₂ spike
721 suggests manifold reactions were removing this form before reaching the instruments.” The residence time
722 in the RAMIX manifold was on the order of 1s depending on sampling point and there is no known
723 chemistry that can account for oxidation of Hg(0) or reduction of RGM on this timescale. We would
724 suggest that the most reasonable explanation of the discrepancies between the various RAMIX
725 measurements includes both instrumental artifacts and an incomplete characterization of the RAMIX
726 manifold. If fast gas-phase chemistry is producing or removing RGM in the RAMIX manifold the same
727 chemistry must be operative in the atmosphere as a whole and this requires that we completely revise our
728 current understanding of mercury chemistry. The discrepancies between the DOHGS and speciation
729 systems are further indication that artifacts are associated with KCl denuder sampling under ambient
730 conditions but we would suggest that RAMIX does not constitute an independent verification of the
731 DOHGS performance and that the 2P-LIF measurements raise questions about the DOHGS measurements.

732 Ambrose et al. (2013) also suggest that the observations of very high RGM concentrations indicate
733 multiple forms of RGM and that the concentrations can be explained by oxidation of Hg(0), with O₃ and
734 NO₃ being the likely nighttime oxidants. We have discussed these reactions in detail previously (Hynes et
735 al., 2009) and concluded that they cannot play any role in homogeneous gas phase oxidation of Hg(0).
736 Ambrose et al. (2013) cite recent work on this reaction by Rutter et al. (2012) stating that “On the basis of

737 thermodynamic data for proposed reaction mechanisms, purely gas-phase Hg(0) oxidation by either O₃ or
738 NO₃ is expected to be negligibly slow under atmospheric conditions; however, in the case of O₃-initiated
739 Hg(0) oxidation, the results of laboratory kinetics studies unanimously suggest the existence of a gas-phase
740 mechanism for which the kinetics can be treated as second-order.” We would suggest that a careful reading
741 of the cited work by Rutter et al. (2013) demonstrates the opposite conclusion. We provide additional
742 discussion of these issues in the SI and again conclude that O₃ and NO₃ can play no role in the
743 homogeneous gas phase oxidation of Hg(0).

744

745 **5.0 Future Mercury Intercomparisons**

746 The discrepancies that are discussed above suggest a need for a careful independent evaluation of
747 mercury measurement techniques. The approaches used during the evaluation of instrumentation for the
748 NASA Global Tropospheric Experiment (GTE) and the Gas-Phase Sulfur Intercomparison Experiment
749 (GASIE) evaluation offer good models for such an evaluation. The Chemical Instrument and Testing
750 Experiments (CITE 1-3) (Beck et al., 1987; Hoell et al., 1990; Hoell et al., 1993) were a major component
751 of GTE establishing the validity of the airborne measurement techniques used in the campaign. The GASIE
752 experiment (Luther and Stetcher, 1997; Stetcher et al., 1997) was a ground based intercomparison of SO₂
753 measurement techniques that might be particularly relevant to issues associated with mercury measurement.
754 In particular, GASIE was a rigorously blind intercomparison that was overseen by an independent panel
755 consisting of three atmospheric scientists, none of whom were involved in SO₂ research. We would suggest
756 that a future mercury intercomparison should be blind with independent oversight. Based on the RAMIX
757 results it should consist of a period of direct ambient sampling and then manifold sampling in both reactive
758 and unreactive configurations. For example, an unreactive configuration would consist of Hg(0) and
759 oxidized mercury in an N₂ diluent eliminating any possibility of manifold reactions and offering the
760 possibility of obtaining a manifold blank response. Such a configuration would allow the use of both
761 denuder and pyrolysis measurements since it is reasonable to conclude, based on the current body of
762 experimental evidence, that denuder artifacts are associated with ambient sampling with water vapor and
763 ozone as the most likely culprits. A reactive configuration would be similar to the RAMIX manifold
764 configuration with atmospheric sampling into the manifold and periodic addition of Hg(0) and oxidized
765 mercury over their ambient concentrations. The combination of the three sampling configurations should
766 enable instrumental artifacts to be distinguished from reactive chemistry in either the manifold itself or, for
767 example, on the KCl denuder.

768

769 **6.0 Conclusions**

770 We deployed a 2P-LIF instrument for the measurement of Hg(0) and RGM during the RAMIX campaign.
771 The Hg(0) measurements agreed reasonably well with instruments using gold amalgamation sampling
772 coupled with CVAFS analysis of Hg(0). Measurements agreed to within 10-25% on the short term
773 variability in Hg(0) concentrations based on a 5 minute temporal resolution. Our results also suggest that

774 the operation of the RAMIX manifold and spiking systems were not as well characterized as Finley et al.
775 (2013) suggest. We find that the calculated concentration spikes consistently overestimated the amount of
776 Hg(0) introduced into the RAMIX manifold by as much as 30%. This suggests a systematic error in
777 concentration calculations rather than random uncertainties that should not produce a high or low bias.

778 We made measurements of TM, and hence TOM by difference, by using pyrolysis to convert
779 TOM to Hg(0) and switching between pyrolyzed and ambient samples. The short term variation in ambient
780 Hg(0) concentrations is a significant limitation on detection sensitivity and suggests that a two channel
781 detection system, monitoring both the pyrolyzed and ambient channels simultaneously is necessary for
782 ambient TOM measurements. Our TOM measurements were normally consistent, within the large
783 uncertainty, with KCl denuder measurements obtained with two Tekran speciation systems and with our
784 own manual KCl denuder measurements. The ability of the pyrolysis system to measure higher RGM
785 concentrations was demonstrated during one of the manifold HgBr₂ spikes but the results did not agree with
786 those reported by the UW DOHGS system. We would suggest that it is not possible to reconcile the
787 different measurement approaches to TOM. While there is other evidence that KCl denuders may
788 experience artifacts in the presence of water vapor and ozone, the reported discrepancies cannot explain the
789 very large differences reported by the DOHGS and Tekran speciation systems. Similarly, the differences
790 between the DOHGS and 2P-LIF pyrolysis measurements suggest that one or both of the instruments were
791 not making reliable, quantitative measurements of RGM. We suggest that instrumental artifacts, an
792 incomplete characterization of the sampling manifold, and limitations in the measurement protocols all
793 make significant contributions to the discrepancies between the different instruments and that it would be
794 rash to draw significant implications for the atmospheric cycling of mercury based on the RAMIX results.
795 This is particularly true of the RGM results. If one were to conclude that the discrepancies between the
796 DOHGS and speciation systems sampling ambient oxidized mercury are accurate and reflect a bias that can
797 be extrapolated to global measurements then it means that atmospheric RGM concentrations are much
798 higher than previously thought and that we have little understanding of the atmospheric cycling of mercury.
799 What is not in dispute is the urgent need to resolve the discrepancies between the various measurement
800 techniques. The RAMIX campaign provided a valuable guide for the format of any future mercury
801 intercomparison. It clearly demonstrated the need to deploy high accuracy calibration sources of Hg(0) and
802 oxidized mercury, the need for multiple independent methods to measure elemental and oxidized mercury
803 and to clearly characterize and understand the differences reported by instruments that are currently being
804 deployed for measurements.

805

806 **Acknowledgements**

807 This work was supported by NSF Grant # AGS-1101965, a National Science Foundation Major
808 Instrumental Grant (#MRI-0821174) and by the Electric Power Research Institute. We thank Mae Gustin
809 and her research group and Robert Novak for their hospitality, assistance and use of laboratory facilities

810 during the RAMIX intercomparison. We thank Mae Gustin and Dan Jaffe for the use of their RAMIX data
811 for comparison with our results. We thank Eric Prestbo for helpful comments on the manuscript.

812

813

814 **References:**

815 Ambrose, J. L.; Lyman, S. N.; Huang, J.; Gustin, M. S.; Jaffe, D. A.: Fast time resolution oxidized mercury
816 measurements during the Reno Atmospheric Mercury Intercomparison Experiment (RAMIX), *Environ.*
817 *Sci. Technol.*, 47 (13), 7284–7294; DOI 10.1021/es303916v, 2013.

818

819 Bauer, D.; Campuzano-Jost, P.; Hynes, A. J., Rapid, ultra-sensitive detection of gas phase elemental
820 mercury under atmospheric conditions using sequential two-photon laser induced fluorescence, *J. Environ.*
821 *Monitor.*, 4, (3), 339-343, 2002.

822

823 Bauer, D., D’Ottone, L., Campuzano-Jost, P. and Hynes, A. J.: Gas Phase
824 Elemental Mercury: A Comparison of LIF Detection Techniques and
825 Study of the Kinetics of Reaction with the Hydroxyl Radical, *J. Photochem.*
826 *Photobio*, 57, 247, 2003

827

828 Bauer, D., Everhart, S., Remeika, J., Tatum Ernest, C., and Hynes, A. J.: Deployment of a Sequential Two-
829 Photon Laser Induced Fluorescence Sensor for the Detection of Gaseous Elemental Mercury at Ambient
830 Levels: Fast, Specific, Ultrasensitive Detection with Parts-Per-Quadrillion Sensitivity, *Atmos. Meas.*
831 *Tech.*, 7, 4251-4265, www.atmos-meas-tech-discuss.net/7/5651/2014/ doi:10.5194/amtd-7-5651-2014,
832 2014.

833

834 Breckenridge, W. H. and Umemoto, H.: Collisional Quenching of Electronically Excited Metal Atoms, in
835 *Advances in Chemical Physics: Dynamics of the Excited State*, Volume 50 (ed K. P. Lawley), John Wiley
836 & Sons, Inc., Hoboken, NJ, USA. doi: 10.1002/9780470142745.ch5, 2007.

837

838 Beck, S. M.; Bendura, R. J.; Mcdougal, D. S.; et al.: Operational overview of NASA GTE CITE-1 airborne
839 instrument intercomparisons - carbon-monoxide, nitric-oxide, and hydroxyl instrumentation, *J. Geophys.*
840 *Res.*, 92, 1977-1985, 1987

841

842 Díez, S.: Human health effects of methylmercury exposure, *Rev. Environ. Contam. Toxicol.*, 198,
843 111–132, DOI: 10.1007/978-0- 387-09646-9, 2009.

844

845 Ebinghaus, R.; Banic, C.; Beauchamp, S.; Jaffe, D.; Kock, H.; Pirrone, N.; Poissant, L.; Sprovieri, F.;
846 Weiss-Penzias, P., Spatial coverage and temporal trends of land-based atmospheric mercury measurements

847 in the Northern and Southern Hemispheres. In Mercury fate and transport in the global atmosphere:
848 Emissions, measurements and models, Mason, R.; Pirrone, N., Eds. Springer: New York, NY, 2009.
849
850 Ernest, C.T.; Donohoue, D.; Bauer, D.; Ter Schure, A.; Hynes, A.J. Programmable Thermal Dissociation of
851 Reactive Gaseous Mercury, a Potential Approach to Chemical Speciation: Results from a Field Study,
852 Atmosphere, 5, 575-596. doi:[10.3390/atmos5030575](https://doi.org/10.3390/atmos5030575), 2014
853
854 Feng, X.; Lu, J.Y.; Gregoire, D. C.; Hao, Y.; Banic, C. M.; Schroeder, W. H. : Evaluation and application:
855 of a gaseous mercuric chloride source, Anal. Bioanal. Chem., 376, 1137-1140, 2003.
856
857 Finley, B. D.; Jaffe, D. A.; Call, K.; Lyman, S.; Gustin, M.; Peterson, C.; Miller, M.; Lyman, T. :
858 Development, testing, and deployment of an air sampling manifold for spiking elemental and oxidized
859 mercury during the Reno Atmospheric Mercury Intercomparison Experiment (RAMIX). Environ. Sci.
860 Technol., 44, 7277-7284,
861 DOI 10.1021/es304185a, 2013
862
863 Gustin, M.; Jaffe, D., Reducing the Uncertainty in Measurement and Understanding of Mercury in the
864 Atmosphere. Environ. Sci. Technol., 44, (7), 2222-2227, 2010.
865
866 Gustin, M. S.; Huang, J.; Miller, M. B.; Peterson, C.; Jaffe, D. A.; Ambrose, J.; Finley, B. D.; Lyman, S.
867 N.; Call, K.; Talbot, R.; Feddersen, D.; Mao, H.; Lindberg, S. E. Do we understand what the mercury
868 speciation instruments are actually measuring? Results of RAMIX. Environ. Sci. Technol., 47 (13), 7295–
869 7306; DOI 10.1021/es3039104, 2013.
870
871 Hoell, J. M. ; Albritton, D. L.; Gregory, G. L.; et al., Operational overview of NASA GTE/CITE-2 airborne
872 instrument intercomparisons - nitrogen-dioxide, nitric-acid, and peroxyacetyl nitrate, J. Geophys. Res., 95
873 10047-10054, 1990
874
875 Hoell, J. M. ; Davis, D. D.; Gregory, G. L.; et al., operational overview of the NASA GTE CITE-3 airborne
876 instrument intercomparisons for sulfur-dioxide, hydrogen-sulfide, carbonyl sulfide, dimethyl sulfide, and
877 carbon-disulfide, J. Geophys. Res., 98, 23291-23304, 1993.
878
879 Houyoux, M.; Strum, M. Memorandum: Emissions Overview: Hazardous Air Pollutants in Support of the
880 Final Mercury and Air Toxics Standard; EPA-454/R-11-014; Emission Inventory and Analysis Group Air
881 Quality Assessment Division: Research Triangle Park, NC, USA, 2011.
882 Available at: <http://www.epa.gov/mats/pdfs/20111216EmissionsOverviewMemo.pdf>
883

884 Hynes, A. J.; Donohoue, D. L.; Goodsite, M. E.; Hedgecock, I. M., Our current understanding of major
885 chemical and physical processes affecting mercury dynamics in the atmosphere and at the air-
886 water/terrestrial interfaces In *Mercury Fate and Transport in the Global Atmosphere*, Mason, R.; Pirrone,
887 N., Eds. Spring New York, NY, 2009.

888

889 Landis, M. S.; Stevens, R. K.; Schaedlich, F.; Prestbo, E. M., Development and Characterization of an
890 Annular Denuder Methodology for the Measurement of Divalent Inorganic Reactive Gaseous Mercury in
891 Ambient Air. *Environ. Sci. Technol.*, 36, (13), 3000-3009, 2002.

892

893 Lin, C.J.; Pongprueksa, P.; Lindberg, S.E.; Pehkonen, S.O.; Byun, D.; Jang, C. Scientific uncertainties in
894 atmospheric mercury models I: Model science evaluation. *Atmos. Environ.*, 40, 2911–2928,
895 doi:10.1016/j.atmosenv.2006.01.009, 2006.

896

897 Lindberg, S. E.; Bullock, R.; Ebinghaus, R.; Engstrom, D.; Feng, X.; Fitzgerald, W.; Pirrone, N.; Prestbo,
898 E.; Seigneur, C. A synthesis of progress and uncertainties in attributing the sources of mercury in
899 deposition. *Ambio*, 36, 1932, 2007.

900

901 Luther III, D. W.; D.L.; Stecher, H.A. III, Preface: Historical background. *J. Geophys. Res.*, 102, 16215-
902 16217, 1997.

903

904 Lyman, S. N.; Jaffe, D. A.; Gustin, M. S. Release of mercury halides from KCl denuders in the presence of
905 ozone. *Atmos. Chem. Phys.* 2010, 10, 8197–8204; DOI 10.5194/acp-10- 8197- 2010.

906 Mason, R.A. Mercury Emissions from Natural Processes and their Importance in the Global Mercury
907 Cycle. In *Mercury Fate and Transport in the Global Atmosphere: Emissions, Measurements and Models*;
908 Pirrone, N., Mason, R.A., Eds.; Springer: Dordrecht, The Netherlands, 2009; pp. 173–191.

909

910 Mergler, D.; Anderson, H.A.; Chan, L.H.M.; Mahaffey, K.R.; Murray, M.; Sakamoto, M.; Stern, A.H.
911 Methylmercury exposure and health effects in humans: A worldwide concern. *Ambio* 2007, 36, 3–11,
912 doi:10.1579/0044-7447(2007)

913

914 McClure, C. D.; Jaffe, D.A.; Edgerton, E.S. Evaluation of the KCl denuder method for gaseous oxidized
915 mercury using HgBr₂ at an in-service AMNet site. | *Environ. Sci. Technol.* 2014, 48, 11437–11444,
916 dx.doi.org/10.1021/es502545k

917

918 Prestbo, E. C., Air Mercury Speciation Accuracy and Calibration, SFO Air Mercury Speciation Workshop,
919 July 2014. Available at <http://omicsgroup.com/conferences/ACS/conference/pdfs/14958-Speaker-Pdf-T.pdf>
920

921 Prestbo, E. C., Chief Scientist, Tekran Instruments, personal communication, 2015.
922
923 Pirrone, N.; Cinnirella, S.; Feng, X.; Finkelman, R.B.; Friedli, H.R.; Learner, J.; Mason, R.; Mukherjee,
924 A.B.; Stracher, G.; Streets, D.G.; Telmer, K. Global mercury emissions to the atmosphere from natural and
925 anthropogenic sources. In *Mercury Fate and Transport in the Global Atmosphere: Emissions,*
926 *Measurements and Models*; Pirrone, N., Mason, R.A., Eds.; Springer: Dordrecht, The Netherlands, 2009;
927 pp. 3–50.
928
929 Rutter, A.P., Shakya, K.M., Lehr, r., Schauer, J. J., Griffin, R. J., Oxidation of gaseous elemental mercury
930 in the presence of secondary organic aerosols, *Atmos. Environ.*, 59, 86-92, 2012
931
932 Scheuhammer, A.M.; Meyer, M.W.; Sandheinrich, M.B.; Murray, M.W., Effects of environmental
933 methylmercury on the health of wild bird, mammals, and fish. *Ambio* 2007, 36, 12–18, doi:10.1579/0044-
934 7447(2007)36[12:EOEMOT]2.0.CO;2.
935
936 Selin, N.E., Global Biogeochemical Cycling of Mercury: A Review. *Annu. Rev. Environ. Resour.* 2009,
937 34, 43–63, doi:10.1146/annurev.envIRON.051308.084314.
938
939 Slemr, F., Brunke, E.-G., Ebinghaus, R., and Kuss, J.: Worldwide trend of atmospheric mercury since
940 1995, *Atmos. Chem. Phys.*, 11, 4779-4787, doi:10.5194/acp-11-4779-2011, 2011.
941
942 Slemr, F.; Weigelt, A.; Ebinghaus, R.; Kock, H.H.; Bödewadt, J.; Brenninkmeijer, C.A.M.; Rauthe-Schöch,
943 A. ; Weber, S.; Hermann, M.; Zahn, A.; Martinsson, B.; Atmospheric mercury measurements onboard the
944 CARIBIC passenger aircraft, *Atmos. Chem. Phys.*, accepted for publication, 2016
945
946 Sprovieri, F., Pirrone, N., Bencardino, M., D'Amore, F., Carbone, F., Cinnirella, S., Mannarino, V., Landis,
947 M., Ebinghaus, R., Weigelt, A., Brunke, E.-G., Labuschagne, C., Martin, L., Munthe, J., Wängberg, I.,
948 Artaxo, P., Morais, F., Barbosa, H. D. M. J., Brito, J., Cairns, W., Barbante, C., Diéguez, M. D. C., Garcia,
949 P. E., Dommergue, A., Angot, H., Magand, O., Skov, H., Horvat, M., Kotnik, J., Read, K. A., Neves, L.
950 M., Gawlik, B. M., Sena, F., Mashyanov, N., Obolkin, V., Wip, D., Feng, X. B., Zhang, H., Fu, X.,
951 Ramachandran, R., Cossa, D., Knoery, J., Maruscak, N., Nerentorp, M., and Norstrom, C.: Atmospheric
952 mercury concentrations observed at ground-based monitoring sites globally distributed in the framework of
953 the GMOS network, *Atmos. Chem. Phys.*, 16, 11915-11935, doi:10.5194/acp-16-11915-2016, 2016.
954
955 Streets, D.G.; Devane, M.K.; Lu, Z.; Bond, T.C.; Sunderland, E.M.; Jacob, D.J. All-time releases of
956 mercury to the atmosphere from human activities. *Environ. Sci. Technol.* 2011, 45, 10485–10491.
957

958 Stecher, H.A. III; Luther III, G.W.; MacTaggart, D.L.; Farwell, S.O.; Crossley, D.R.; Dorko, W.D.;

959 Goldan, P.D.; Beltz, N.; Krischke, U.; Luke, W.T.; Thornton, D.C.; Talbot, R.W.; Lefer, B.L.; Scheuer,

960 E.M.; Benner, R.L.; Wu, J.; Saltzman, E.S.; Gallagher, M.S.; Ferek, R.J.: Results of the gas- phase sulfur

961 intercomparison experiment (GASIE): Overview of experimental setup, results, and general conclusions, J.

962 Geophys. Res., 102, 16219-16236, 1997

963

964 Subir, M.; Ariya, P. A.; Dastoor, A. P., A review of uncertainties in atmospheric modeling of mercury

965 chemistry I. Uncertainties in existing kinetic parameters : Fundamental limitations and the importance of

966 heterogeneous chemistry. Atmos. Environ., 45, 5664-5676, 2011.

967

968 Subir, M.; Ariya, P.A.; Dastoor, A.P. A review of the sources of uncertainties in atmospheric mercury

969 modeling II. Mercury surface and heterogeneous chemistry—A missing link. Atmos. Environ. 2012, 46, 1–

970 10, doi:10.1016/j.atmosenv.2011.07.047.

971

972 Swartzendruber, P. C.; Jaffe, D. A.; Finley, B.:Improved fluorescence peak integration in the Tekran 2537

973 for applications with sub-optimal sample loadings, Atmos. Environ., Volume 43, 3648-3651, 2009

974

975 UNEP, United Nations Environment Program, Chemicals Branch, Mercury, Time to Act, 2013

976

977 UNEP, United Nations Environment Program, Chemicals Branch, The Global Atmospheric Mercury

978 Assessment: Sources, Emissions and Transport, 2008.

979

980 UNEP, United Nations Environment Program: <http://www.mercuryconvention.org>, 2014

981

982 U.S. EPA, United States Environmental Protection Agency “Mercury Research Strategy”, EPA/600/R-

983 00/073, , September 2000.

984

985 U.S. EPA, United States Environmental Protection Agency, [Mercury and Air Toxics Standard](http://www.epa.gov/mats). Available

986 online: <http://www.epa.gov/mats> (accessed on 13 March 2013).

987

988

989

990

991

992 Table 1: RAMIX Manual KCl Denuder Sampling

Date	Sample	mid	sample	blank		time	spec1		spec2

	time	point							(uncorr	
	hours	hour	pg m ⁻³	pg m ⁻³			GOM	PBM	GOM	PBM
							pg m ⁻³	pg m ⁻³	pg m ⁻³	pg m ⁻³
9/6	1.5	15	127.9*	2.27		13:00	200.7	51.8	205.1	4.3
						15:00	65.7	32.0	84.9	6.0
9/7	2	16	112.9*	0		14:00	39.8	136.4	94.3	2.5
			21.2			16:00	48.5	177.3	68.9	1.5
			285.8*			18:00	28.1	182.2	37.4	3.3
			30.6							
9/10	3	15.3	74.3	1995		14:00	26.7	10.5	27.4	4.2
			44.2			16:00	24.1	18.3	23.7	2.3
9/13	4	15	12.8	8.2		13:00	0.7	16.9	0.5	16.6
			13.56			17:00	37.6	16.1	25.2	2.7
9/14	4.5	14	39*	3.3		12:00	34.9	12.0	23.9	5.5
			17.3			14:00	57.	18.4	26.3	38.6
						16:00	42.0	17.4	26.3	4.0
9/15	4.5	15	15.24	1.53		13:00	113.9	39.1	27.6	3.9
			20.4	4.87		15:00	80.6	22.2	17.7	3.9
						17:00	110.8	24.1	8.6	8.1
9/16	2.75	16	148*	5		8:00	19.7	4.7	14.8	5.4
			42	6		9:00				
			26	5		10:00	28.7	13.3	19.9	4.8
			47	4						

993

- * evidence from TDPs for presence of PBM

994

- Measurements for UNR Speciation system made at similar times. The Spec 2 measurements are

995

uncorrected values.

996

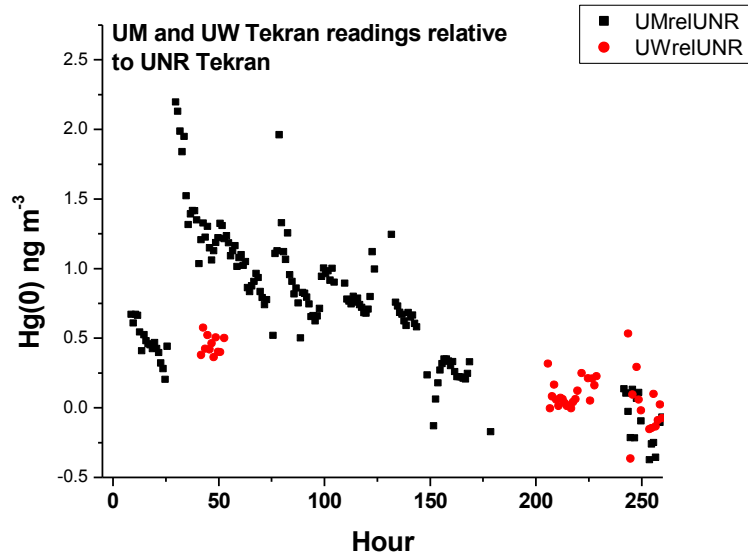
997

998

999

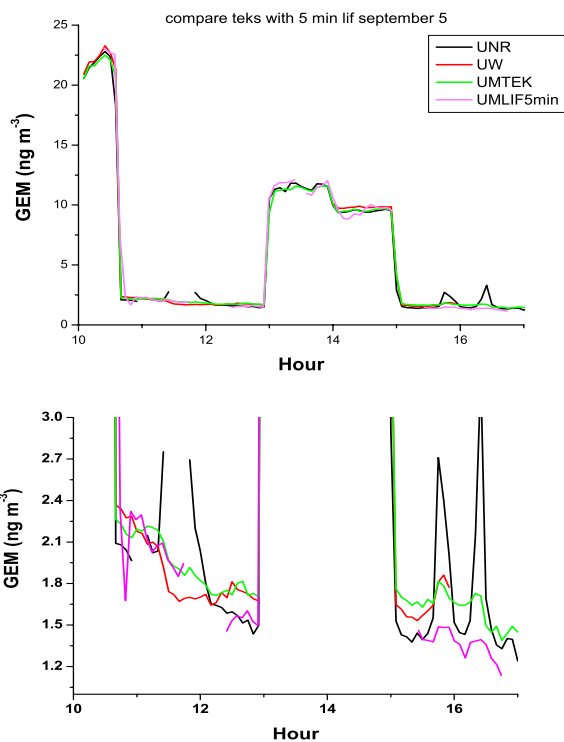
1000
1001
1002
1003
1004
1005
1006
1007
1008
1009
1010
1011
1012

Figures.



1013
1014
1015
1016

Figure 1. Comparison of Hg(0) readings from the UM, UW and UNR Tekrans over the first 260 hours of UM measurements. The absolute concentration difference relative to the UNR instrument is shown in black for the UM Tekran and in red for the DOHGS (UW) Tekran.



1017

1018 Figure 2: a). A seven hour sequence of GEM measurements from September 5th that included two manifold

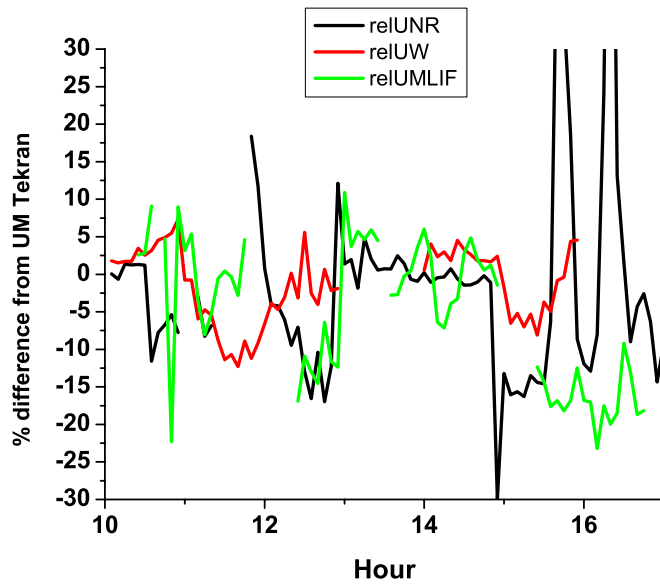
1019 spikes. Shown are the sequence of GEM measurements from the UNR, UW and UM Tekrans together with

1020 the 5 minute averages of the 2P-LIF signal. b) An expanded concentration scale focusing on ambient

1021 measurements.

1022

1023



1024

1025

1026 Figure 3: Seven hour measurement period from September 5th. The % difference of the UNR (black line)

1027 and UW (red line) Tekrans and the UM 2P-LIF (blue line) measurements relative to the UM Tekran is

1028 shown.

1029

1030

1031

1032

1033

1034

1035

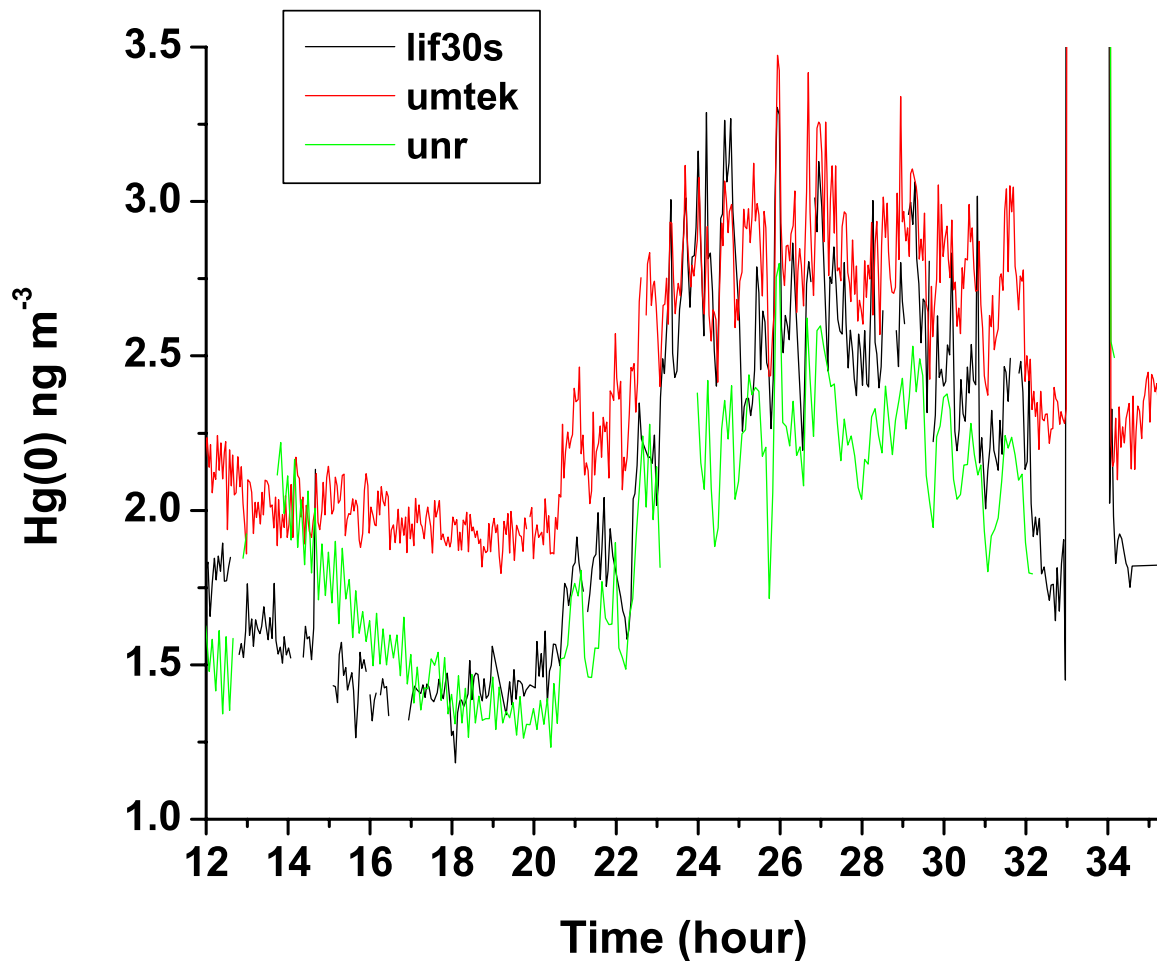
1036

1037

1038

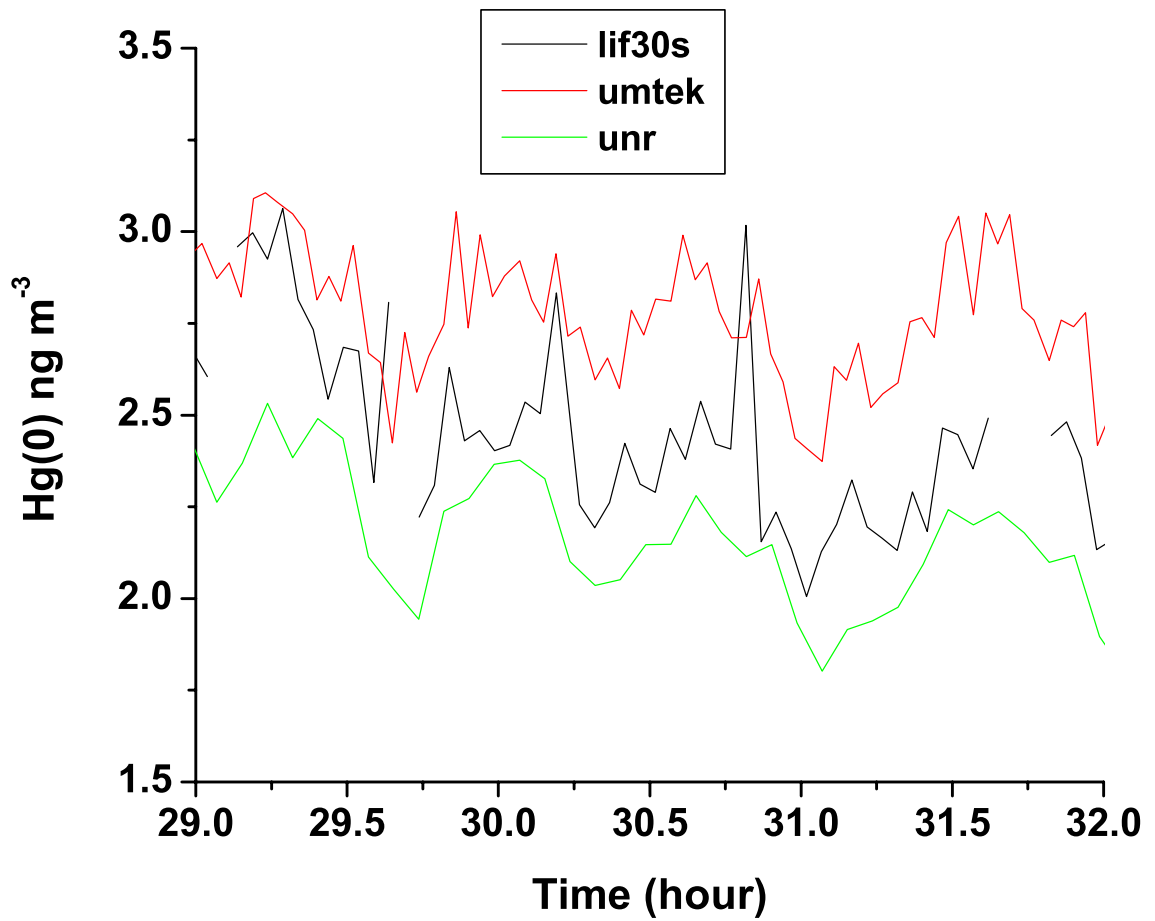
1039

1040



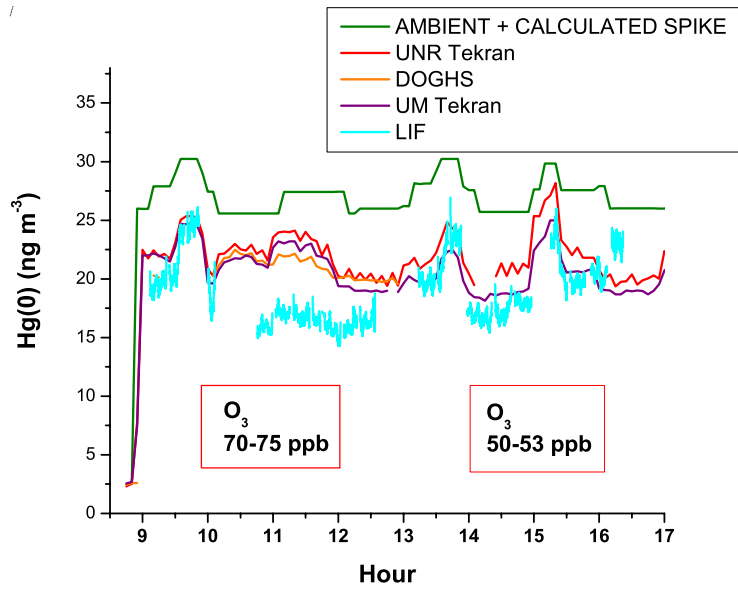
1041
 1042
 1043
 1044
 1045
 1046
 1047
 1048
 1049
 1050
 1051
 1052
 1053
 1054

Fig 4: 22 hour sampling period from September 1st and 2nd. Comparison of the UM (red line) and UNR (green line) Tekrans with the UM 2P-LIF (black line) concentrations. The concentrations for each instrument are scaled to force agreement during the second manifold spike at hour 33. This is the data from SI Fig. 3 with the concentration scale expanded to shown only ambient data.



1055
 1056
 1057
 1058
 1059
 1060
 1061
 1062
 1063
 1064
 1065
 1066

Fig 5: A section of the 22 hour sampling period from September 1st and 2nd. Comparison of the UM (red line) and UNR (green line) Tekrans with the UM 2P-LIF (black line) concentrations. The concentrations for each instrument are scaled to force agreement during the second manifold spike at hour 33. This is the data from SI Fig. 3 with the concentration scale expanded to shown only ambient data between hours 29 and 32.



1067

1068

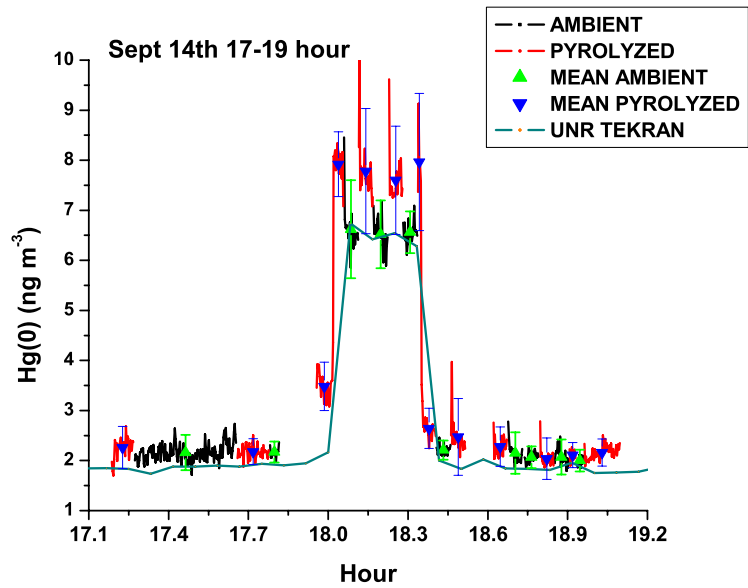
1069 Figure 6: September 7th an ozone interference test. A comparison of the UM, UW and UNR Tekrans and

1070 the UM-2P-LIF measurements. The “expected” concentration calculated from the ambient Hg(0)

1071 concentration prior to the spike plus the calculated spike concentration is also shown.

1072

1073

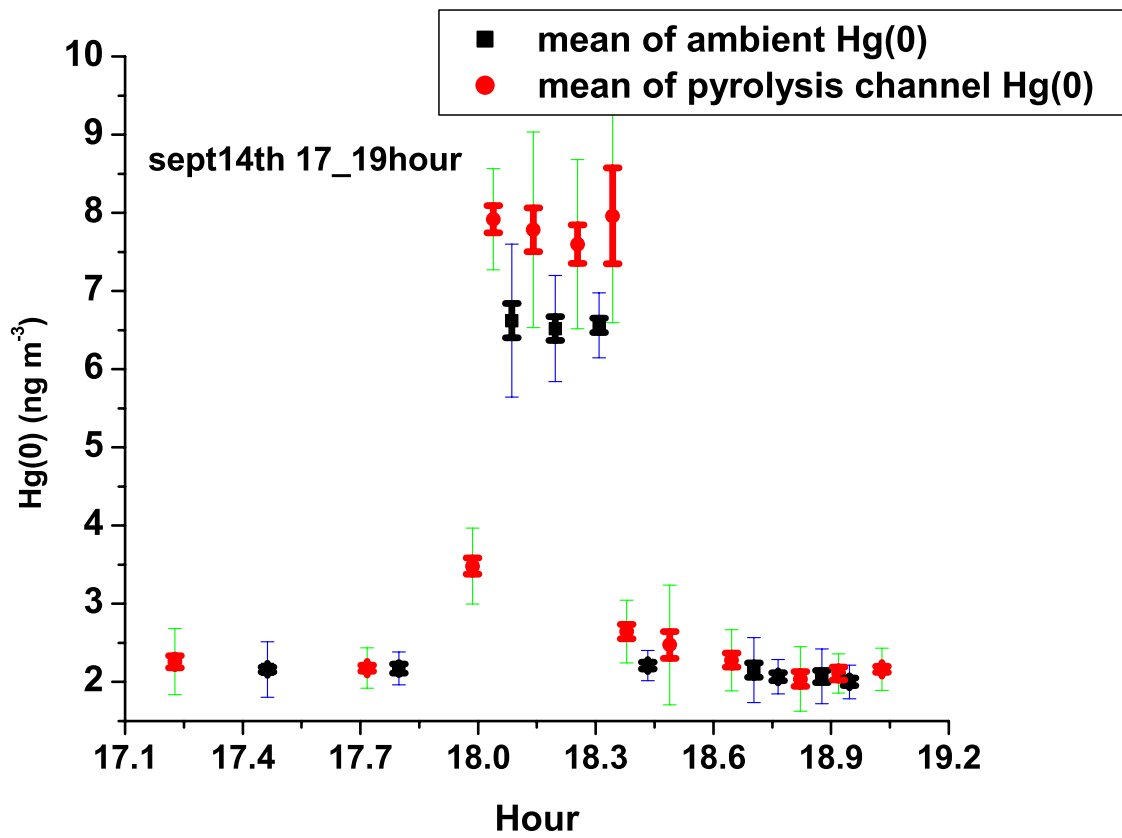


1074

1075

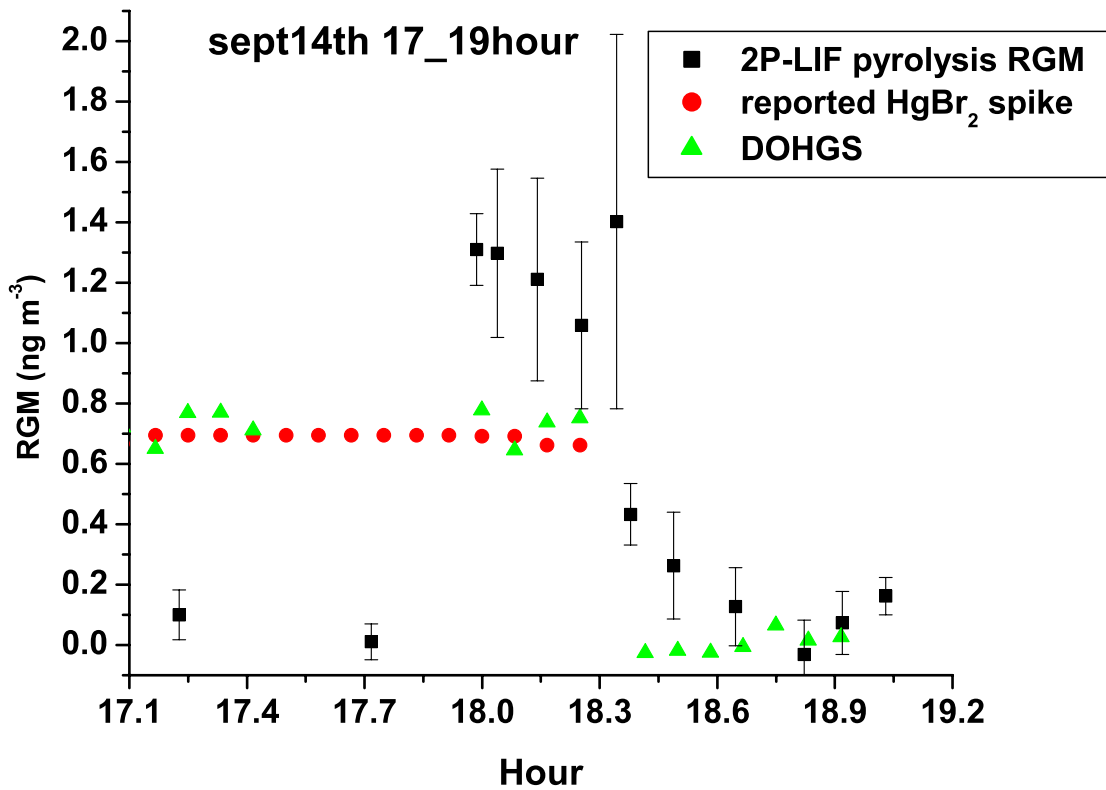
1076 Fig 7: September 14 measurements, hours 17-19 (5-7pm). The background subtracted 2P-LIF signals from
 1077 the ambient (black) and pyrolyzed (red) sampling lines are shown. The gaps correspond to times when the
 1078 laser was blocked to check power and background. The means and 1 standard deviation of each sample are
 1079 shown. The absolute Hg(0) concentrations are obtained by scaling the ambient Hg(0) signal to the absolute
 1080 Hg(0) concentration reported by the UNR Tekran during the Hg(0) manifold spike.

1081



1082
 1083
 1084
 1085
 1086
 1087

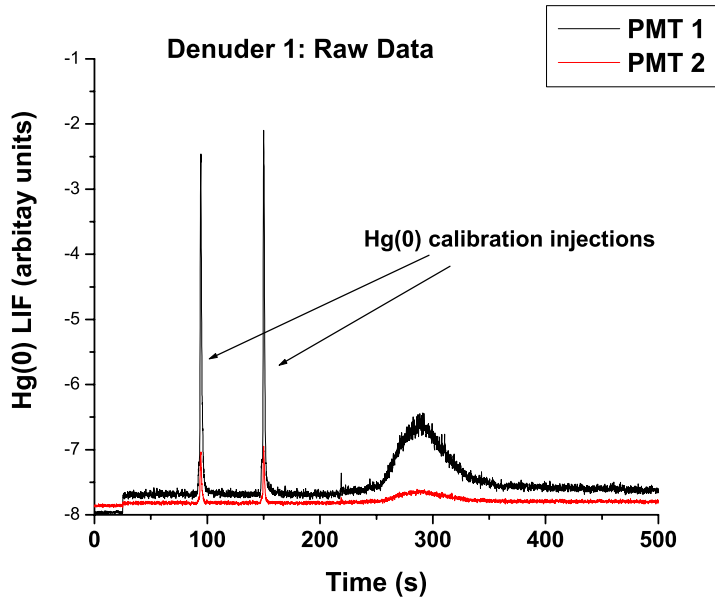
Fig. 8: September 14 measurements, hour 17-19. The means of the ambient channel (black) and pyrolyzed channel (red) are shown. The error bars show both 2 standard errors (thicker line) and 2 standard deviations.



1088
 1089
 1090
 1091
 1092
 1093
 1094

Fig 9: TOM concentrations calculated from the difference between the pyrolyzed and ambient sample concentrations together with 2SE in the TOM concentrations. The reported HgBr₂ spike concentrations and DOHGS measurements are also shown.

1095



1096

1097

1098 Fig. 10: September 16th KCl manual denuder measurements. The raw data for the temporal decomposition

1099 profiles (TDP) for the denuder D1 is shown.

1100

1101

1102

1103

1104

1105

1106

1107

1108

1109

1110

1111

1112

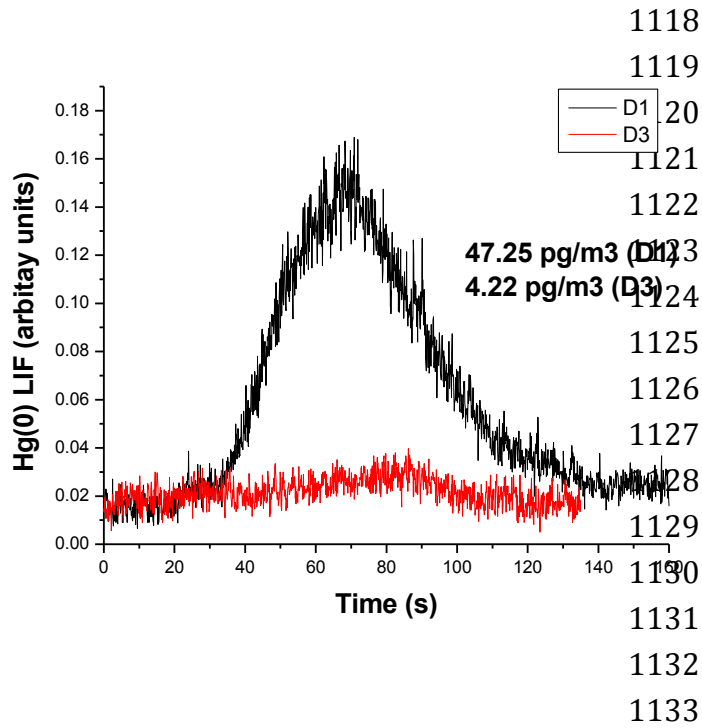
1113

1114

1115

1116

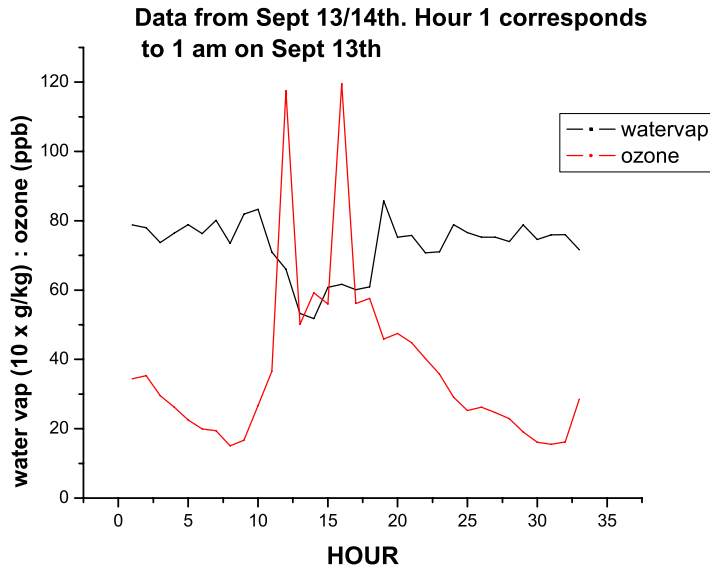
1117



1134 Fig. 11 September 16th KCl manual denuder measurements. The calibrated temporal decomposition profiles
1135 (TDP) for the tandem denuder pair, D1 and D3 are shown.

1136
1137
1138
1139
1140
1141
1142
1143
1144
1145
1146
1147
1148
1149
1150
1151
1152
1153
1154

1155



1156

1157

1158

1159 Fig. 12: The ozone concentration and absolute humidity for a 35 hour sampling period on September 13th

1160 and 14th that included two ozone spikes and only sampled ambient TOM.

1161

1162

1163

1164

1165

1166

1167

1168

1169

1170

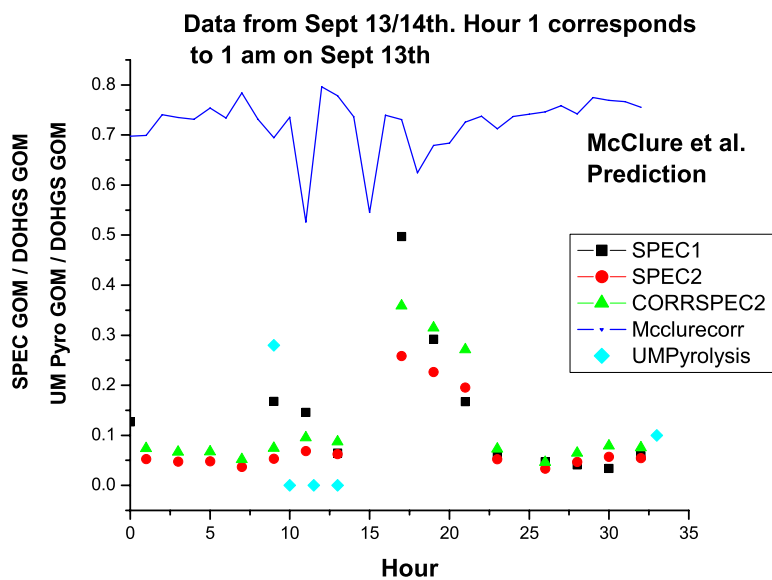
1171

1172

1173

1174

1175



1176
 1177
 1178
 1179
 1180
 1181
 1182
 1183
 1184
 1185
 1186
 1187
 1188
 1189
 1190
 1191
 1192
 1193
 1194
 1195
 1196
 1197
 1198
 1199

Fig. 13. Expected denuder recovery based on the formula determined by McClure et al. which varies between a typical value of ~70% dropping to ~50% during the ozone spikes. The figure also shows the reported recoveries, i.e. the ratio of RGM as measured by either the UNR speciation systems or the 2P-LIF system divided by the value reported by the DOHGS system.

1200

1201

1202